THESIS

ASSESSING AND UNDERSTANDING THE GENERATION AND FUNCTION OF RNA DECAY INTERMEDIATES IN NON-INSECT BORNE FLAVIVIRUSES

Submitted by

Cary T. Mundell

Graduate Degree Program in Cell and Molecular Biology

In partial fulfillment of the requirements

For the Degree of Master of Science

Colorado State University

Fort Collins, Colorado

Summer 2019

Master's Committee:

Advisor: Jeffrey Wilusz

Brian Geiss
Rushika Perera
Anireddy Reddy

ABSTRACT

ASSESSING AND UNDERSTANDING THE GENERATION AND FUNCTION OF RNA DECAY INTERMEDIATES IN NON-INSECT BORNE FLAVIVIRUSES

Cellular gene expression is an intricate process regulated on many levels that allows the cell to react correctly to stimuli or to maintain homeostasis. RNA viruses must act to preferentially drive production of their own messenger RNAs (mRNAs) and proteins in order to successfully replicate and ensure continued infection. Due to the necessity for RNA viruses to remain in the cytoplasm, regulatory factors that affect host mRNAs likely also affect the transcripts of RNA viruses. RNA decay represents a major pathway of regulation for mRNAs. A multitude of RNA viruses possess unique mechanisms that act to prevent the decay of viral transcripts and allow for successful translation. Members of the viral family *Flaviviridae* are positive sense, single-stranded RNA viruses that do not possess a poly(A) tail. Therefore, it is highly likely that these transcripts would be marked as deadenylated and shuttled down one of the RNA decay pathways that exist in the cell. Interestingly, members of the genera *Flavivirus* of the family *Flaviviridae* possess a conserved structured 3' untranslated region (UTR) that acts to interfere with the decay processes of the major cytoplasmic cellular 5'-3' decay enzyme XRN1. In addition, members of the generas *Hepacivirus,* Hepatitis C Virus (HCV) and *Pestivirus*, Bovine Viral Diarrhea Virus (BVDV), possess XRN1 stalling elements within their 5' UTRs. These stalling sites block the action of the exonuclease and generate decay intermediates. The generation of these decay intermediates represses XRN1 activity in the infected cell.

Herein we demonstrate a new method for studying RNA decay through the use of XRN1-resistant RNAs (xrRNAs). In this method we utilize the well characterized xrRNA of Dengue Virus Type 2 (DENV2) as a readout to study the decay rates of relatively large RNA constructs. We show that not only is utilizing an xrRNA an effective method for confirming XRN1-mediated decay, but that the accumulation of the readout xrRNA can be utilized to understand changes in the decay kinetics of RNA substrates. We further utilize this method to demonstrate a lack of XRN1 stalling elements within the poliovirus internal ribosomal entry site (IRES) element. We provide evidence that the stalling of XRN1 in the 5' UTR of BVDV is dependent on both the presence of the entire IRES structure and the presence of a stem loop 5' to the IRES element through the analysis of a series of truncations. Finally, we demonstrate one possible role for the HCV and BVDV decay intermediates as the truncated IRES element maintains translatability in an *in vitro* system. Collectively, these data better define the structural requirements for the novel XRN1 stalling elements located in the 5' UTR of non-insect borne members of the *Flaviviridae* as well as the potential function of the decay intermediates.

ACKNOWLEDGEMENTS

I would first like to thank Dr. Phillida Charley for her guidance when I first arrived, and for her invaluable assistance as I learned the techniques necessary to this body of work. I would like to thank Dr. Joe Russo, for being an excellent source of encouragement over the course of my degree. I would like to thank John Anderson for being a sounding board for many ideas presented herein. I would like to thank the other members of the Jeff Wilusz lab, Tavo, and Dr. Daniel Michalski for their assistance and support. I would like to thank Adam Heck for showing me the ropes when I arrived for the first time at CSU. I would like to thank Carol Wilusz for giving me a chance to participate in this program as well as being a font of wisdom and reason over the course of my graduate career. I am truly thankful for the opportunities granted to me by Dr. Jeff Wilusz. The enthusiasm he possessed towards my success has driven me and allowed me to grow far beyond what I thought myself capable. I would like to thank my family and friends for their unwavering support and encouragement. Amanda- Thank you for staying with me through this process, and being a constant source of encouragement, optimism, and for forcing me to get out of bed in the morning, without you this would not have been possible.

TABLE OF CONTENTS

LIST OF FIGURES

Introduction

Members of the *Flaviviridae* cause many medically relevant diseases in both humans and animals.

The family *Flaviviridae* consists of 3 genera of single-stranded positive sense RNA viruses, *Flaviviruses, Hepaciviruses, and Pestiviruses.* Genus *Flavivirus* consists of many arthropod-borne viruses that are transmitted primarily by mosquitos and ticks. Members of this genus include many well-known viruses, such as Zika virus, West Nile virus and Dengue Virus Type 2 (DENV2), that all represent potential health care crises across the planet. DENV in particular is amongst the most medically relevant as approximately 1/3 of the world's population is at risk for DENV infection[1]. In addition, these viruses present major threats to both human and animal health due in part to their propensity to rapidly spread to new geographic regions. Unfortunately, there are limited vaccination options to prevent flavivirus infections, the most efficacious being the attenuated YF-VAX yellow fever vaccine. There is an available vaccine, Dengyaxia, for Dengue viruses, however its utility has recently been questioned, and West Nile and Zika viruses lack a vaccine at all[2]. As such, it is of critical importance that further treatments for these diseases be investigated. The best way to begin these investigations is to fully understand the molecular aspects of infections with these nucleic acid pathogens.

Genera *Hepacivirus,* contains one relevant virus to this study, Hepatitis C Virus (HCV). HCV is a virus that has infected an estimated 143 million worldwide as of 2015[3]. HCV causes a chronic infectious disease that leads to a variety of liver conditions over the course of a long infection. While there are successful treatments for HCV that were recently developed[4], there are unfortunately no vaccines for HCV. The challenge of preventing HCV infections, in

combination with its asymptomatic nature and the expense of post-exposure treatments, leave a need for continued research into understanding the mechanisms of HCV-host interactions during infection. This was one of two major goals of this project.

The last virus of importance to this study is a member of the genera *Pestiviruses*, Bovine Viral Diarrhea Virus (BVDV) is a major agricultural pest with a prevalence rate in cattle stocks as high as 80% in Europe and as high as 50% in the United States[5,6] One major challenge of BVDV to herd owners is that calves are often trans-placentally infected, leading to an inability to remove the virus from the calves' system. These persistently infected calves become continuous shedders of the virus and are thus a risk to the herd as a whole. It is estimated that as of 2011 BVDV cost cattle owners $400 per head of infected cattle[7]. As such there is a vested economic interest in understanding how BVDV is evading cellular defenses. Understanding an aspect of BVDV interaction with one of these defenses – the cellular RNA decay machinery – was the other major goal of this thesis project.

RNA Decay Pathways are Critical to Proper Gene Expression Profiles of Cells

All eukaryotic cells possess mechanisms for the regulation of quality and quantity of messenger RNAs[8]. The cellular mRNA decay machinery is a major part of this process. Once an mRNA is targeted for decay it can be shuttled down multiple potential pathways for degradation. There is deadenylation-independent decay, endonuclease-mediated decay, nonsense-mediated decay, and two deadenylation-dependent pathways, either 5'-3' decay, or 3'-5' decay[8,9,10]. All of the pathways play a vital role in the control of both the quality and quantity of mRNA and will be discussed herein.

First, we will examine one of the less common pathways of decay, endonuclease-mediated decay. Fragments of mRNAs produced by endonuclease-mediated decay undergo degradation in both the 5'-3' pathway, mediated by XRN1, and the 3'-5' decay pathway, mediated by the RNA exosome[8]. There are a variety of endonucleases that exist within the realm of mRNA decay, including PMR1, IRE1, RNase MRP, and AGO. All three of these endonucleases act to cleave targeted mRNAs into smaller fragments. PMR1 is a polysome-associated endonuclease involved in the destabilization of albumin mRNA in *X. laevis*[11–13]. Interestingly, PMR1 targets actively translating mRNAs due to the location of PMR1 on the polysome. IRE1 also happens to target actively translating mRNAs as part of the ER stress response in *D. melanogaster*[14] and other organisms. RNase MRP has previously been shown to be involved in the processing of rRNAs and mitochondrial RNAs[15]. Recent studies have also implicated this enzyme in the process of degrading the CLB2 mRNA towards the end of mitosis[16]. Also of interest are short interfering RNAs (siRNAs) and micro RNAs (miRNAs) that initiate endonucleolytic decay through the Argonaute (AGO) 2 protein[17,18].

In addition to endonuclease-mediated decay, there are decay pathways that act to surveil mRNAs for aberrant transcripts and ensure they are removed from the pool of translatable mRNAs. One example of these is that of Non-Stop Decay (NSD), a decay process that targets transcripts that lack a stop codon[9,19,20]. Transcripts that fit this description can be generated due to a variety of reasons, including the natural absence of an in-frame stop codon or mRNA breakage. Currently there exists two potential pathways for NSD, the first pathway involves the exosome, the SKI2/SKI3/SKI8 complex and SKI7[19,20]. Currently it is believed that a stalled ribosome on an NSD RNA substrate is released due to the ribosome binding with the C-terminus of SKI7. Next SKI7 recruits the exosome and the SKI2/3/8 complex to promote deadenylation

and decay through 3'-5' degradation[19,20]. If however SKI7 is not present, for example in *S. cerevisiae*, 5'-3' decay pathway can be engaged in the NSD pathway, potentially due to the removal of poly(A) binding protein (PABP) from the mRNA transcript by the ribosome[21].

The process of Nonsense-Mediated Decay (NMD) is a major surveillance system that cells utilize to classically recognize and degrade transcripts that have suboptimal positioning of their termination codons[10]. Often these termination codons are 50-55nt upstream of an exon junction, but recent studies have located targets of NMD that do not possess premature termination codons[22,23]. The major proteins involved in the targeting of mRNAs for NMD are the UPF family of proteins, UPF1, UPF2, and UPF3. UPF1 is considered the primary NMD factor due to its centrality at most steps of the NMD process. UPF1 is present for most, if not all, of the steps of NMD from recognition of RNAs destined for degradation to the final degradation of these RNAs[10]. While many details of the process by which translation termination activates NMD is differentiated from standard translation termination are still relatively unknown, it is clear that the eukaryotic release factors are critical in the process due to their ability to recognize the termination codon[10]. The current models of NMD posit that UPF1 is recruited to the terminating ribosome through a direct interaction with eRF3[23] causing the formation of a specific complex on the transcript. There is some discussion in the field with regards to the association of PABP and how it might prevent the formation of the eRF3-UPF1 complex and thus prevent NMD from occuring[24,25]. However, recent evidence suggests that PABP needs to interact with eIF4G and that eIF4G is responsible for the antagonization of NMD.[26,27]

After UPF1 and eRF3 associate, a downstream protein complex assembles which leads to the activation of NMD. The order in which this occurs is not well understood, but it is generally thought that there is a ribosome-associated complex that consists of eRF1-3, DHX34, UPF1, and

SMG1C (a complex consisting of SMG1, a kinase, and SMG1's regulators SMG8 and 9).[24,28,29] This complex is potentially responsible for translation termination and for the prevention of the initiation of further translation. SMG1-mediated phosphorylation of UPF1 acts to recruit the mRNA degradation machinery at this point as well[28,30]. Now that the degradation machinery has been recruited, there are four potential mechanisms for the degradation of RNA. First, the SMG6 endonuclease can be recruited to cleave mRNAs proximal to the premature termination codon followed be subsequent RNA degradation by the RNA exosome and XRN1. Second, a SMG-7 heterodimer can be recruited which in turn recruits the CCR4-NOT deadenylase complex, leading to shortening of the poly(A) tail and subsequent targeting for decapping.[31,32] Third, PRNC2 can be recruited which then allows for recruitment of the general decapping complex. Finally, the general decapping complex can be recruited directly to the targeted mRNA. All of these decapping steps are generally followed by degradation by the 5'-3' exonuclease XRN1.

In terms of mRNA turnover, XRN1 is best known in conjunction with RNA decay brought about due to decapping of mRNAs targeted for degradation. This pathway is one of the two possible results of deadenylation-based decay, the most common pathway of mRNA decay in cells. The stability of mRNAs generally depends on modifications to their 5' and 3' termini - a variable length 3' poly(A) tail and a 5' 7-methylguanosine cap. These features interact with cytoplasmic proteins to coordinate protection from roaming exonucleases[9,33]. As previously mentioned, it is possible for nucleases to attack these RNAs if these structures are removed or through an endonucleolytic cleavage event that generates accessible ends. In the case of deadenylase-mediated decay, the trip to destruction begins with the removal of the poly(A) tail from the mRNA in question. Interestingly, this step is not necessarily irreversible, as certain mRNAs/ developmental situations allow for readenylation and relocalization to polysomes[34].

Once an mRNA has been targeted for deadenylation, one of several deadenylases leap into action and proceed to deadenylate the mRNA through a variety of mechanisms. Generally, the PAN2-PAN3 complex is the first to act by shortening the tail of mRNAs to ~80 nucleotides in both mammalian cells and in *S. cervesiae*[32,35]. At this point the CCR4-NOT deadenylase takes over and proceeds to trim the poly(A) tail even further, forcing disassociation of PABP1 from the 3' end of the mRNA and allowing for the LSM1-7 complex to bind[36]. The mRNAs are now shuttled down to their ultimate fate, either they will be targeted for 3'-5' decay or they will be decapped and degraded from the 5' end by XRN1.

In eukaryotes, 3'-5' decay appears to be largely mediated by a complex of proteins known as the exosome. The eukaryotic exosome is similar to that of the archaeal exosome but is more complex by far[37–39]. The core of the exosome is comprised of a pseudo-hexameric ring that is formed by 3 heterodimeric protein pairings, MTR3-RRP42, RRP41-RRP45, RRP46-RRP35, that have structural similarities to the archaeal PNPase PH-1 and PH-2 domains[40]. This hexameric ring contains enough space to allow for the positioning of one single stranded RNA. Once the RNA is in place, XRN1 initiates progressive phosphorlytic activity catalyzing the removal of nucleotides in a sequential pattern until the mRNA is degraded. Once the RNA is degraded, the scavenger enzyme DCPS arrives and proceeds to separate the 5' 7mG cap from the resulting short RNA fragments[41].

If the deadenylated RNA is targeted for degradation down the 5'-3' pathway, decapping must first occur and then XRN1 can proceed to degrade the mRNA. As the mRNA is deadenylated, PABP1 is no longer associated with the mRNA, destabilizing the binding of eIF4E to the 7mG cap[42]. Additionally, the deadenylated mRNA is bound by the LSM1-7 complex of proteins, which in turn stabilizes the interaction of the Dcp1/2 complex which is

instrumental in removal of the 7mG cap. Dcp1/2 is a holoenzyme with Dcp2 acting as the catalytic subunit. The Dcp ½ complex acts to cleave the 7mG cap off of the mRNA through hydrolysis, yielding a m7GDP and a 5' monophosphate residue on the now decapped transcript[43]. This 5' monophosphate residue is perhaps the most important outcome of the entire degradation process, as XRN1 cannot effectively degrade RNA substrates that do not possess this feature[44]. The XRN1 N-terminus exists as a highly conserved nuclease domain, surrounded by 5 other conserved regions: a PAZ/Tudor domain, a SH3-like domain, a KOW domain, and a winged helix domain[44]. The SH3 domain and the PAZ/Tudor domains exist to stabilize the confirmation of XRN1to facilitate nuclease activity[33,44]. The KOW domain is classified as an RNA-binding domain[45]. The winged-helix domain has multiple potential functions, including the mediation of protein-protein interactions, shielding the entry site of XRN1, and the ability to stabilize the RNA-protein complex by directly interacting with RNA strands[44]. Unfortunately, the C-terminus of XRN1 is not as well understood as its N-terminus. A proline-rich region has been identified that appears to act to stabilize the interaction between the decapping complex and XRN1 in humans and in *Drosophila*[46,47].

Crystallization of the XRN1 N-terminus bound to an RNA reveals that the 5' phosphate is inserted into a basic pocket that excludes larger triphosphates or 7mG cap structures[44] and allows only for recognition of 5' monophosphate residues through electrostatic interactions. This specific recognition of the 5' terminal nucleotide allows for processive degradation down the substrate after each successive hydrolysis[44]. This processivity allows for rapid clearance of mRNAs destined for degradation. This is not to say, however, that XRN1 is unstoppable once it has located a proper substrate. In fact, there exist RNA structures that are very refractory to the activity of XRN1.

Members of the *Flaviviridae* Interfere with Host mRNA Decay Pathways

As members of the *Flaviviridae* are single stranded RNA viruses, the endogenous cellular mRNA decay machinery may very well play the role of a first line defense mechanism. In fact flavivirus RNAs are perhaps primed for mRNA decay due to their inherent lack of a poly(A) tail[48,49]. However, while flavivirus RNAs are clearly subject to 5'-3' exoribonuclease-mediated decay, they also possess a highly structured region in one of their UTRs that interferes with the processive decay of the XRN1 enzyme. Arthropod-borne flaviviruses possess a conserved 3' UTR three helix junction structure that is utilized to both inhibit XRN1 progression along the RNA substrate as well as to repress XRN1 activity in a reversible fashion[50–53]. The three-helix junction is created through the stacking of RNA helices on one another to form a ring-like structure. The 5' end of the XRN1-resistant RNA (xrRNA) is then pulled through the ring, establishing the structure that XRN1 encounters in the course of degrading flaviviral RNAs. In addition, there is evidence that some flavivirus 3' UTRs have the potential to form a pseudoknot structure that strengthens the formation of the three-helix junction.[54] This composition prevents XRN1 from effectively degrading the rest of the RNA, but also settles in the active site of the RNA, preventing immediate disengagement from these XRN1 resistant RNAs[50,52,55,56]. This stalling and temporary repression of XRN1 activity is one mechanism that flaviviruses utilize to prevent degradation of their mRNAs.

3' UTR XRN1 stalling sites were also recently found in other virus families, notably *Benyviridae*[57], *Phlebovirus*[53], *Dianthrovirus*[58], and the *Arenaviridae*[53] . This commonality of this strategy among virus families is an interesting development in the viral-host arms race. However, 3' UTR structures are not the only approach to XRN1 interference present in viral RNAs. HCV and BVDV, two non-insect borne flaviviruses, both possess RNA structures in their

5’ UTRs that stall XRN1[59]. These stall sites precede the core of the Internal Ribosome Initiation Site (IRES) elements present in the 5’ UTR of these viruses. IRES elements are of distinct importance for HCV and BVDV as they allow the naturally uncapped viral transcripts to be efficiently translated.

IRES elements act to allow uncapped viruses to initiate translation through a variety of means. There are currently four groups of IRES elements classified, with both HCV and BVDV belonging to Group 2. These IRES elements bind to the 40S subunit of the ribosome and utilize only a small portion of the canonical eukaryotic initiation factors, specifically eIF3 and eIF2, as well as Met-tRNA$_i$[60,61] as shown in Figure 1. In addition, there are pseudoknot interactions upstream of the start codon that are required for initiation of translation.

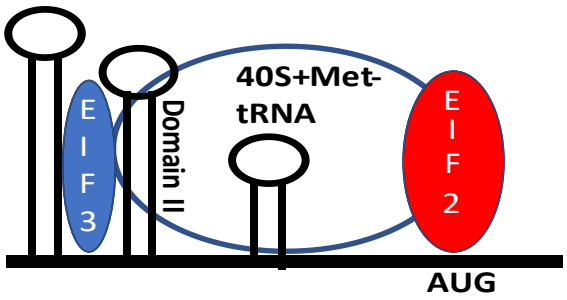

Figure 1. Simplified Diagram of Group 2 IRES Element and Translation Initiation Factors

These IRES elements are critical for the production of viral protein as the virus possesses no other method for initiation of translation. Group 1 IRES elements bind directly to the ribosome and do so independent of any standard translation protein factors, they also do not require methionyl-tRNA$_i$.[62,63] Group 3 IRES elements require some eukaryotic initiation factors, including eIF2,3,4A,4B, and 4G, Met-tRNA$_i$ and a series of IRES transactivating factors[64]. Group 4 IRESs require many of the same factors as Group 3 IRESs, but initiate translation at an AUG relatively downstream of the IRES element when compared to Group 3 IRESs[65]. Group 2

IRES elements like the HCV and BVDV 5' UTRs have extended RNA helices from two folded helical junctions. These helices act as a scaffold for the binding of eIF3 and the 40S subunit as shown in Figure 1[60,66]. In addition, this complex forms independent of other cellular factors[66,67]. Domain II of the HCV IRES contacts the 40S subunit directly at the E site of t-RNA binding[68]. Once this complex forms, the HCV IRES then drives recruitment of eIF3 and the eIF2-Met-tRNA$_i$-GTP complex to form what is known as the 48S*-IRES complex[69,60,70]. This complex proceeds to assemble the 80S ribosomal subunit[69,60,70] and the HCV transcript will now be translated. Interestingly, the 5' UTR stall sites of HCV and BVDV are located upstream of the major regions of the IRES elements in both BVDV and HCV as can be seen in Figure 2.

One pressing question is the possible function of the decay intermediates formed by the stalling of XRN1 around these IRES elements. In this project, we chose to pursue the hypothesis

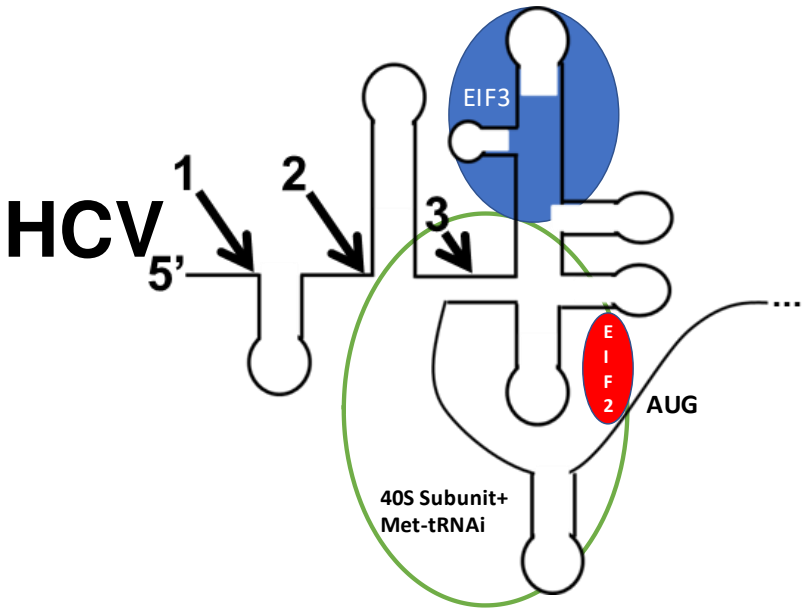

Figure 2- Representative schematic of XRN1 stall sites in context of the HCV IRES structure. Numbers represent approximate XRN1 stall sites and colored shapes represent the translation initiation factors shown in Figure 1.

that the 5' shortened RNA decay intermediates might still be able to serve as translational templates for viral protein synthesis.

Practical application of flaviviral RNA decay intermediates in the study of RNA turnover.

Currently the *in vitro* study of RNA decay and the formation of RNA decay intermediates by the stalling of XRN1 are limited by the inability to resolve large RNA fragments on polyacrylamide gels. We and others hypothesized that XRN1 stalling by xrRNAs might be utilized to generate more informative RNA decay assays, including the establishment of single molecule assays for tracking mRNA decay in live cells.

Previous work on visualizing RNA decay in living cells has focused on utilizing RNA FISH or tagging proteins to use as readouts. These methods are not preferable due to the potential for negative readouts as an RNA decays[71]. However, Horvathova et al. generated a method that instead utilizes the ability of xrRNAs to stall XRN1 to protect a fluorescent probe to use as a readout of decay rates[72]. PP7 bacteriophage stem loops were inserted upstream of the West Nile virus (WNV) xrRNA and a set of MS2 bacteriophage stem loops were placed downstream of the WNV xrRNA. This will allow for tracking of decay of the construct by either XRN1 in a 5-3' manner or decay by the exosome in a 3'-5' manner dependent upon which fluorescent probe was present in tracked RNAs. Intact RNAs would show a signal from both fluorophores[72]. Importantly these constructs have similar translation and turnover profiles as unmodified reporter RNAs.

Use of these constructs demonstrated four interesting findings: First, the evidence gathered by the authors demonstrated that the turnover of mRNA could be modeled utilizing a Poisson distribution, suggesting that decay occurs at independent rates per RNA. Second, RNA

interference was almost exclusively cytoplasmic, and the decay rates of Ago2-mediated endonucleolytic cleaved RNAs was not necessarily tied to the exonucleolytic decay of the fragments. Third, the authors contradicted previous models of mRNA decay occurring within P-bodies. Finally, the authors showed that inhibition of translation stabilizes mRNAs[71,72].

Another recent utilization of xrRNA inclusion technology in living cells is the 'xrFrag' methodology outlined by Boehm et al[73]. The authors generated a construct of the triosephosphate isomerase (TPI) ORF with the Murray Valley Encephalitis (MVE) xrRNA inserted 3' of the stop codon of the RNA substrates. Examination of the construct through northern blot analysis post transfection of cells showed strong buildup of the MVE decay intermediates. This verified that the construct would demonstrate accumulation of the xrRNA to allow for monitoring of decay by XRN1. Next the authors investigated the ability for their construct to be used to track NMD. By inserting a premature termination codon in their construct, they were able to demonstrate that their construct was targeted for NMD and subsequently was degraded by XRN1 as seen by the accumulation of their xrRNA readout. The authors were also able to demonstrate a separation of decapping and endonucleolytic cleavage activities and deadenylation. The successful use of xrRNAs in these two cellular contexts demonstrates the potential power for the use of these XRN1-resistant structures for the improvement of RNA decay assays – and motivated us to see how the inclusion of xrRNA structures into RNA substrates could help with the final readout of biochemically-reconstituted RNA decay reactions.

Materials and Methods

Generation of Templates for RNA Substrates for xrRNA-Modified XRN1 Decay Assays

Templates for *in vitro* transcription to generate radiolabeled RNAs for use in the xrRNA-modified XRN1 decay assays were generated as Geneblocks. The fundamental units of our Geneblock design were an SP6 bacterial promotor sequence followed by the open reading frame of GAPDH and terminating with the DENV2 minimal XRN1 stalling sequence at the 3' end. A schematic of construct design can be seen in figure 3. Various alterations and structural elements to this core experimental design can be found in Table 1 below:

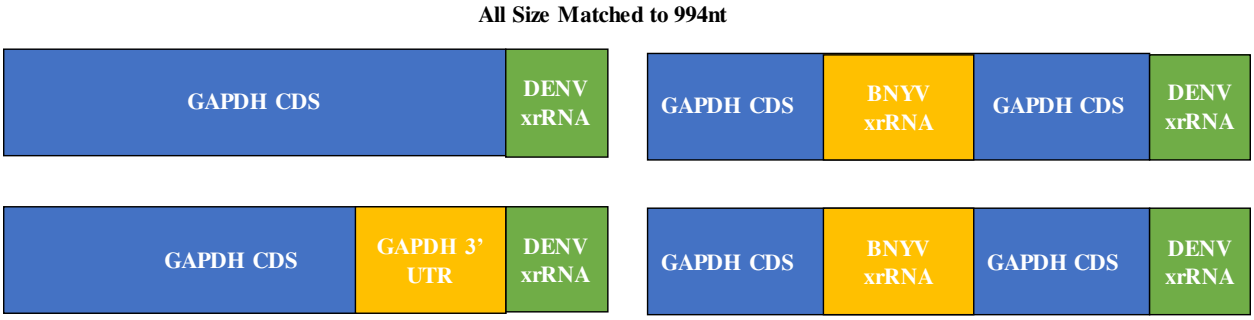

Figure 3. Schematic representation of constructs for modified decay assay

Table 1. Sequences for Geneblocks Used as Templates for *In Vitro* Transcription. The sequence of the SP6 promoter is indicated by the capital letters.

Construct Name	Construct Sequence
GAPCH-CDS	GATCATCGAATTTAGGTGACACTATAGcccttcattgacctcaactacatggtttaca tgttccaatatgattccacccatggcaaattccatggcaccgtcaaggctgagaacgggaagcttgtcatcaatg gaaatcccatcaccatcttccaggagcgagatccctccaaaatcaagtggggcgatgctggcgctgagtacgt cgtggagtccactggcgtcttcaccaccatggagaaggctggggctcatttgcagggggagccaaaagggt catcatctctgccccctctgctgatgcccccatgttcgtcatgggtgtgaaccatgagaagtatgacaacagcct caagatcatcagcaatgcctcctgcaccaccaactgcttagcacccctggccaaggtcatccatgacaactttg gtatcgtggaaggactcatgaccacagtccatgccatcactgccacccagaagactgtggatggcccctccgg gaaactgtggcgtgatggccgcggggctctccagaacatcatccctgcctctactggcgctgccaaggctgtg ggcaaggtcatccctgagctgaacgggaagctcactggcatggccttccgtgtccccactgccaacgtgtcag

	tggtggacctgacctgccgtctagaaaaacctgccaaatatgatgacatcaagaaggtggtgaagcaggcgtc ggagggccccctcaagggcatcctgggctacactgagcaccaggtggtctcctctgacttcaacagcgacac ccactcctccacctttgacgctggggctggcattgccctcaacgaccactttgtcaagctcatttcctggtatgac aacgaatttggctacagcaacagggtggtggacctcatggcccacatggcctccaaggagtaaaaaagaagt caggccatcacaaatgccacagcttgagtaaactgtgcagcctgtagctccacc
GAPDH CDS-3' UTR	GATCATCGAATTTAGGTGACACTATAGccaccatggagaaggctggggctcatttgc agggggggagccaaaagggtcatcatctctgccccctctgctgatgcccccatgttcgtcatgggtgtgaaccat gagaagtatgacaacagcctcaagatcatcagcaatgcctcctgcaccaccaactgcttagcacccctggcca aggtcatccatgacaactttggtatcgtggaaggactcatgaccacagtccatgccatcactgccacccagaag actgtggatggcccctccgggaaactgtggcgtgatggccgcggggctctccagaacatcatccctgcctcta ctggcgctgccaaggctgtgggcaaggtcatccctgagctgaacgggaagctcactggcatggccttccgtgt ccccactgccaacgtgtcagtggtggacctgacctgccgtctagaaaaacctgccaaatatgatgacatcaag aaggtggtgaagcaggcgtcggagggcccccctcaagggcatcctgggctacactgagcaccaggtggtctc ctctgacttcaacagcgacacccactcctccacctttgacgctggggctggcattgccctcaacgaccactttgt caagctcatttcctggtatgacaacgaatttggctacagcaacagggtggtggacctcatggcccacatggcct ccaaggagtaagacccctggaccaccagccccagcaagagcacaagaggaagagagagaccctcactgct ggggagtccctgccacactcagtcccccaccacactgaatctcccctcctcacagttgccatgtagacccctg aagaggggaggggcctagggagccgcaccttgtcatgtaccatcaataaagtaccctgtgctcaaccagttaa agaagtcaggccatcacaaatgccacagcttgagtaaactgtgcagcctgtagctccacc
GAPDH CDS-SL	GATCATCGAATTTAGGTGACACTATAGccccttcattgacctcaactacatggtttaca tgttccaatatgattccacccatggcaaattccatggcaccgtcaaggctgagaacgggaagcttgtcatcaatg gaaatcccatcaccatcttccaggagcgagatccctccaaaatcaagtggggcgatgctggcgctgagtacgt cgtggagtccactggcgtcttcaccaccatggagaaggctggggctcatttgcaggggggagccaaaagggt catcatctctgccccctctgctgatgccccatgttcgtcatgggtgtgaaccatgagaagtatgacaacagcct caagatcatcagcaatgcctcctgcaccaccaactgcttagcacccctggccaaggtcatccatgacaactttg gtatcgtggaaggactcatgaccacagtccatgccatcactgccacccagaagactgtggatggcccctccgg gatatcccgtgagaggggcgcgtcggtggcggctgtttgccgattcgacagccgccacctacgcgccctcg cacgggatatctccctgagctgaacgggaagctcactggcatggccttccgtgtccccactgccaacgtgtca gtggtggacctgacctgccgtctagaaaaacctgccaaatatgatgacatcaagaaggtggtgaagcaggcgt cggagggcccccctcaagggcatcctgggctacactgagcaccaggtggtctcctctgacttcaacagcgaca cccactcctccacctttgacgctggggctggcattgccctcaacgaccactttgtcaagctcatttcctggtatga caacgaatttggctacagcaacagggtggtggacctcatggcccacatggcctccaaggagtaaaaaagaag tcaggccatcacaaatgccacagcttgagtaaactgtgcagcctgtagctccacc
GAPDH CDS-BNYV	GATCATCGAATTTAGGTGACACTATAGccccttcattgacctcaactacatggtttaca tgttccaatatgattccacccatggcaaattccatggcaccgtcaaggctgagaacgggaagcttgtcatcaatg gaaatcccatcaccatcttccaggagcgagatccctccaaaatcaagtggggcgatgctggcgctgagtacgt cgtggagtccactggcgtcttcaccaccatggagaaggctggggctcatttgcaggggggagccaaaagggt catcatctctgccccctctgctgatgccccatgttcgtcatgggtgtgaaccatgagaagtatgacaacagcct caagatcatcagcaatgcctcctgcaccaccaactgcttagcacccctggccaaggtcatccatgacaactttg gtatcgtggaaggactcatgaccacagtccatgccatcactgccacccagaagactgtggatggcccctttggt gtaatcgtccgaagacgttaaactacacgtgatttcacggtgttcggtgagcctctactggcgctgccaaggctg tgggcaaggtcatccctgagctgaacgggaagctcactggcatggccttccgtgtccccactgccaacgtgtc agtggtggacctgacctgccgtctagaaaaacctgccaaatatgatgacatcaagaaggtggtgaagcaggc gtcggagggcccccctcaagggcatcctgggctacactgagcaccaggtggtctcctctgacttcaacagcga cacccactcctccacctttgacgctggggctggcattgccctcaacgaccactttgtcaagctcatttcctggtat

	gacaacgaatttggctacagcaacagggtggtggacctcatggcccacatggcctccaaggagtaaaaaaga agtcaggccatcacaaatgccacagcttgagtaaactgtgcagcctgtagctccacc

In vitro Transcription to Generate RNA Substrates

In vitro transcription to generate RNA substrates for XRN1 decay assays utilized the following protocol. Reactions were assembled according to Table 2 below. After incubation at 37°C for 1-3 hours, reactions were phenol-chloroform extracted and the newly formed radiolabeled RNA was collected by ethanol precipitation using ammonium acetate as the salt to minimize contamination with free nucleotides. RNA products were resuspended in a denaturing gel loading dye (Table 3) and loaded onto a 5% denaturing polyacrylamide gel that was run at 600v for approx. 1 hour. Gels were briefly exposed to preflashed X-ray film and bands were excised and eluted overnight into 400 ul of High Salt Column Buffer (HSCB) (Table 4). The eluted RNAs were phenol-chloroform extracted, concentrated by ethanol precipitation and resuspended in water to a typical concentration of 100,000 cpms per ul.

Table 2 – Constituents of a Standard *In Vitro* Transcription Reaction

Template DNA (Geneblock or PCR generated)	**1 µl (50-200ng)**
SP6 Transcription Buffer (NEB)	**2µl**
rNTPs- (5mM rATP & rCTP, 0.5mM rGTP and rUTP), 5mM GMP	**1µl**
RiboLock RNase Inhibitor	**0.5µl**
rUTP [α-^{32}P] (800 Ci/mmole)	**4.5µl**
SP6 RNA Polymerase	**1 µl**
Total Volume	**10µl**

Table 3- Loading Buffer for RNA Polyacrylamide Gels

Urea RNA loading dye:
12g Urea
0.185g EDTA
12.5µl 1M Tris-HCl pH-7.6
0.006g xylene cyanol (Millipore Sigma X4126)
0.006g bromophenol blue (Acros 115-39-9)
Raise volume to 25mL with ddH_2O

Table 4- HSCB Buffer for Elution of RNA

HSCB buffer
400mM NaCl (Thermo Fisher, S271-3)
25mM Tris-HCl (pH 7.6)
0.1% (w:v) SDS (Thermo Fisher, BP166)

XRN1 Decay Assays

XRN1 decay assays were performed by assembling the reactions as outlined in Table 5. Reactions were incubated at 37°C over a time course. Samples were taken at desired time points and the reaction quenched by placing the sample into 400µl HSCB. Reactions were phenol extracted and RNA products were ethanol precipitated. RNA reaction products were then run on a 5% denaturing gel containing 7M urea. The gels were dried on a gel drier for ~1 hr., exposed to a phosphor screen, and analyzed by phosphorimaging.

Table 5. Constituents of a Typical XRN1 Decay Assay.

XRN1 Decay Assay Component	Volume (scale as required)
RNA Substrate	**~6fmol RNA in 1µl**
NEB Buffer 3	**2µl**
RiboLock RNase Inhibitor	**1µl**
NEB Recombinant XRN1	**1µl**
Nuclease Free ddH_20	**15µl**
Total Volume	**20µl**

Generation of Viral 5' UTR Sequences for Gibson Assembly

In order to generate PCR products for use in UTR mapping studies or for Gibson Assembly to generate RNA substrates for *in vitro* translation, the following viral sequences were used. HCV Accession Number: KP666616.1 and BVDV Accession Number: DQ088995.2

Gibson Assembly

In order to elucidate a potential biological function of 5' UTR HCV and BVDV XRN1 decay intermediates, a series of constructs were generated by Gibson Assembly utilizing XRN1 stall sites derived by Stephanie Moon [59]. All 5' UTRs and sequences representing stable decay intermediates thereof were placed in front of the GFP coding sequence. Fragments were designed using the NEBuilder tool. Gibson fragments were generated utilizing PFU Ultra II polymerase in a PCR reaction following the manufacturer's protocol. PCR products were electrophoresed on agarose gels to both ensure correct fragment size and as a means to purify the fragments via excision of bands from the gel. DNA fragments were then assembled utilizing NEBuilder HiFi DNA Assembly mix per the manufacturer's protocol. Assembled fragments were then

transformed into *E. coli*. Antibiotic resistant colonies were then prepped and sequenced to ensure proper construct creation.

Table 6. Sequence of Primers Used to Generate Gibson Assembly Fragments. Capital letters represent the primer binding site in 5' UTR sequence, lowercase letters represent the overhand region necessary for Gibson Assembly.

Gibson Fragment	Fwd Primer Sequence	Rev Primer Sequence
HCV Full	ctcgtagaccgtgcaccatgGTGAGCAAGGGCGAGGAG	gcccccatcaggggctggcTTCTATAGTGTCACCTAAATGGTGGCGACCGGTGGATC
HCV GFP	gggatccaccggtcgccaccATTTAGGTGACACTATAGAAGCCAGCCCCCTGATGGGG	agctcctcgcccttgctcacCATGGTGCACGGTCTACGAGACC
H2	ctcgtagaccgtgcaccatgGTGAGCAAGGGCGAGGAG	gacagtagttcctcacagggTTCTATAGTGTCACCTAAATGGTGGCGACCGGTGGATC
H2 GFP	gggatccaccggtcgccaccATTTAGGTGACACTATAGAAGTGAGGAACTACTG	agctcctcgcccttgctcacCATGGTGCACGGTCTACG
H3	ctcgtagaccgtgcaccatgGTGAGCAAGGGCGAGGAG	tatggctctcccgggaggggTTCTATAGTGTCACCTAAATGGTGGCGACCGGTGGATC
H3 GFP	gggatccaccggtcgccaccATTTAGGTGACACTATAGAACCCCTCCCGGGAGAGCCA	agctcctcgcccttgctcacCATGGTGCACGGTCTACGAGACC
BVDV Full	catggagttgatcacaaatgGTGAGCAAGGGCGAGGAG	cgtatacgagaagggcgaatTTCTATAGTGTCACCTAAATGGTGGCGACCGGTGGATC
BVDV GFP	gggatccaccggtcgccaccATTTAGGTGACACTATAGAAATTCGCCCTTCTCGTATAC	agctcctcgcccttgctcacCATTTGTGATCAACTCCATG
BVDV 1	catggagttgatcacaaatgGTGAGCAAGGGCGAGGAG	tcttttcggccttcgctgagTTCTATAGTGTCACCTAAATGGTGGCGACCGGTGGATC
BVDV 1 GFP	gggatccaccggtcgccaccATTTAGGTGACACTATAGAACTCAGCGAAGGCCGAAAAG	agctcctcgcccttgctcacCATTTGTGATCAACTCCATGTGC
BVDV 2	catggagttgatcacaaatgGTGAGCAAGGGCGAGGAG	atccaacgaactcaccactgTTCTATAGTGTCACCTAAATGGTGGCGACCGGTGGATC

BVDV 2 GFP	gggatccaccggtcgccaccATTTAGGTG ACACTATAGAACAGTGGTGAGT TCGTTGG	agctcctcgcccttgctcacCATTTGTGATCA ACTCCATG

Generation of Capped and Uncapped RNAs for *In Vitro* Translation Assays

Plasmid DNA garnered from Gibson assemblies was linearized and utilized as templates for *in vitro* transcription to generate two types of RNAs substrates for each construct. A 5' 7mGpppG capped and an uncapped (5' ppp) RNA were generated for each Gibson construct to allow for testing of retention of IRES mediated translation function. To generate sufficient RNA for *in vitro* translation, the Sp6 Megascript kit was used following manufacturers protocol with 1 addendum: the generation of capped RNA necessitated a 10:1 ratio of 7mG cap to GTP in the transcription reaction to ensure that capped RNAs would be generated. RNAs were then purified by phenol extraction and ethanol precipitation (in the presence of ammonium acetate to minimize the precipitation of unincorporated nucleotides) to be used as translation templates.

***In Vitro* Translation, Immunoprecipitation and Western Blotting**

RNAs generated as described above were used as templates for translation in the Promega Rabbit Reticulocyte Lysate (RRL) System. To detect the GFP translation product, we utilized an immune-precipitation/western blotting approach to enrich for the translation product of interest. Thus, after a 90 minute incubation in the RRL system, the lysate solution was resuspended in 250µl of radioimmunoprecipitation assay (RIPA) buffer, precleared by incubation with Surebeads Protein A magnetic beads for 1 hr., then the magnetic beads were removed from the lysate and lysate was incubated with the GFP primary Antibody (Table 7) for 1 hour. Antibody-protein complexes were collected using Surebeads Protein G magnetic beads

for 1 hr. The magnetic G beads were resuspended in 50µl of 2x SDS-PAGE protein loading dye and 50µl ddH_20 (Table 8), samples were boiled for 5 minutes, and loaded onto a 10% SDS-PAGE gel. Samples were run at 100v for approximately 1 hour. Gels were then transferred onto PVDF membrane, blocked with 5% milk for one hour, then primary antibody was added at a 1:1000 concentration and incubated overnight. Blots were washed 3x with PBS-T and then placed in 5% milk with secondary antibody (Table 7) at 1:1000 dilution for 1 hour. Blots were washed 3x with PBS-T and 1x with PBS, and then developed with SuperSignal West Dura Extended Duration Substrate and imaged on the Azure Sapphire Biomolecular Imager.

Table 7: Antibodies Used in this Study

Primary Antibody	GFP Monoclonal Antibody, eBiosciences 14-6674-82. Mouse
Secondary Antibody	Mouse TrueBlot Ultra: Anti-Mouse Ig HRP

Table 8: 2x SDS-Page Sample Loading Buffer Recipe

2x Sample Loading Buffer	
1M Tris-HCL pH 6.8	**1ml**
10% SDS	**4ml**
Glycerol	**2ml**
1% Bromophenol Blue	**500µl**
ddH_20	**To 10ml**
Immediately before use, add 1M DTT to a final concentration of 50mM	**Take 950µl of 2x Loading buffer Add 50µl of DTT**

Generation of BVDV 5' UTR 3' Truncations for Mapping

Generation of 3' truncations was generated utilizing a PCR reaction using PFU Ultra II Polymerase per manufacturer's recommendations using the following primers (Table 9).

Table 9: Primers Utilized to Generate BVDV Truncations for Mapping

Forward Primer 5'-3'	
BVDV+Sp6 promoter	ATTTAGGTGACACTATAGAAATTCGCCCTT
Reverse Primers 5'-3'	
BVDV 5' UTR -50nt	TTGTGATCAACTCCATGTGC
BVDV 5' UTR -100nt	CAGTGGGCCTCTGCAGCA
BVDV 5' UTR -150nt	GAACTGCTTTTACCTGGGCG
BVDV 5' UTR -200nt	CATGCCCTCGTCCACGTG
BVDV 5' UTR -250nt	CCACTGACGACTACCCTGTAC
BVDV 5' UTR -300nt	CACTGCTGCTACCCCCCTCT

Results

The inclusion of an XRN1 stalling site in RNA substrates improves and imparts versatility to cell-free RNA decay assays

While *in vitro* RNA decay assays using cellular extracts have been around for over two decades, they have two key limitations in terms of the RNA substrate that is used. First, smaller RNAs are preferred to work with due to the resolving power of acrylamide gels. Second, it is oftentimes difficult to *a priori* discern random degradation by contaminating environmental ribonucleases from *bona fide* cellular RNA turnover. Therefore, we set out to engineer RNA substrates to help address both of these concerns.

As a major limitation of *in vitro* decay assays is the resolution of decay intermediates, Carol Wilusz proposed that we might be able to address this by inserting a sequence that stalls XRN1 near the end of a target RNA substrate. This would allow for a clearly resolvable decay intermediate on the gel that would afford a determination of a couple of key factors. First, it would provide important confirmation that observed RNA substrate decay was indeed due to XRN1 decay and not a contaminating endoribonuclease. Next, it would allow us to quantitatively evaluate XRN1 decay kinetics in larger, more biologically relevant mRNAs. Thus, we embarked on a series of experiments to validate this approach.

We designed four separate constructs to generate mRNA-sized (~1000 bases) RNA substrates with specific sequence content to ascertain XRN1 decay kinetics. The first construct designed was our backbone RNA substrate that provided us with a baseline for XRN1-mediated RNA decay kinetics in our system. We chose the GAPDH coding sequence (GAPDH-CDS) to provide this baseline since it is a housekeeping mRNA and serves as a common normalization standard for many of the *in vivo* assays in our laboratory. To stall XRN1 near the 3' end of the this GAPDH-CDS RNA substrate, we chose to insert the well-characterized xrRNA sequence of

the Dengue Virus type 2 (DENV2) sub-genomic flavivirus RNA (sfRNA)[55]. Note that all of the constructs designed to validate the system contained the DENV2 sfRNA XRN1 stalling site in the same location at their 3' end.

The second construct we designed was to test a hypothesis that 3' untranslated regions might inherently interfere with XRN1 more than other mRNA regions due to a report that they have a propensity to be more structured[74]. We generated this RNA substrate by simply adding the 3' UTR of the GAPDH mRNA to the GAPDH-CDS construct, removing an appropriate number of bases from the 5' side of the open reading frame to ensure that the new RNA substrate (GAPDH CDS-3' UTR) was sized match with the control CDS-containing RNA substrate.

For the last two constructs we opted to insert structures into the CDS region of the GAPDH-CDS construct that might impede the movement of XRN1 and thus slow down the kinetics of RNA decay in our system. We inserted the xrRNA sequence from the Beet Necrotic Yellow Vein Virus (BNYVV) that we recently characterized[57] into the middle of our GAPDH CDS construct (GAPDH-CDS-BNYV) to assess how often XRN1 stalls at the structure and determine how XRN1 decay kinetics are altered by a known stalling site. In essence, this construct served as a positive control for XRN1 stalling at internal sites on an RNA substrate. Finally, we designed a construct with a strong, artificial 87 base stem loop embedded into the GAPDH-CDS construct to determine the effect that a relatively stable RNA secondary structure would have on XRN1 decay kinetics (GAPDH-CDS SL). Given the fact that XRN1 routinely is thought to readily degrade through highly structured rRNA, we created this construct to generate proof of principle data on the impact of secondary structure elements on XRN1 decay kinetics.

We first examined the decay kinetics of our GAPDH CDS RNA substrate when challenged with XRN1. The RNA substrate was incubated with XRN1, time points were collected at 0, 5, 10, 15, and 20 minutes, and reaction products analyzed on an acrylamide gel. As seen in Fig 4A. (top inset) and B, the input RNA was degraded in an approximately linear fashion over the first five minutes of the time course. The bottom inset of Fig. 4 and panel B shows the concomitant accumulation of the DENV2 XRN1-resistant RNA (xrRNA) reporter RNA. Accumulation of the reporter decay intermediate took ~10 minutes to reach maximal levels. We conclude that the majority of the initiation of XRN1-mediated decay of this RNA substrate occurs within 5 minutes of incubation, but that it takes ~ twice that long to maximize the accumulation of the reporter decay intermediate located ~900 bases downstream of the 5' end of the RNA substrate. These data illustrate the value of the assay as both the initiation of decay as well as the time it takes for the enzyme to reach the 3' portion of the substrate can be assessed in the same reaction.

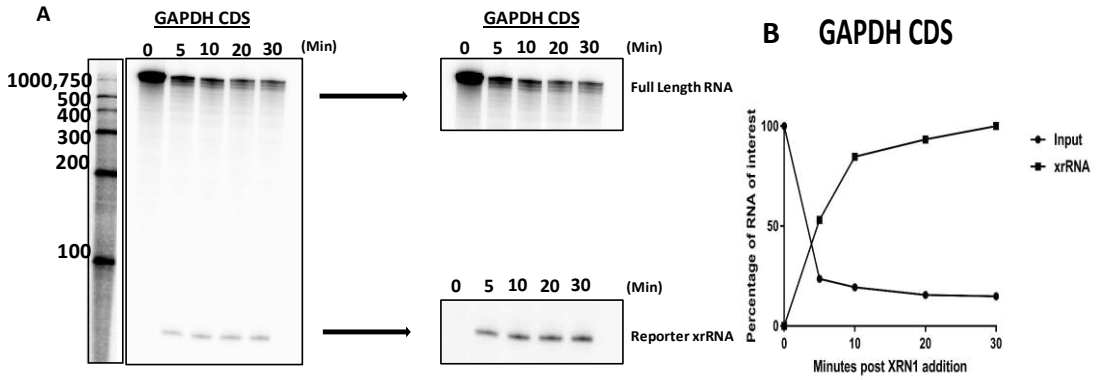

Figure 4. XRN1 decay assay of the GAPDH CDS construct with a time course of 30 minutes. Panel A. Whole image- whole assay to show size of RNAs and size of decay intermediate. Upper inset, Zoom to show input RNA decay. Lower inset, zoom to show reporter xrRNA accumulation. Panel B. The ratio of percent maximal accumulation over time of either the input RNA or reporter xrRNA

We next subjected the GAPDH CDS-3' UTR RNA substrate to XRN1-mediated RNA decay in this system. As seen in Fig. 5, the construct was readily decayed with kinetics qualitatively very similar to the parent GAPDH-CDS construct. From these data we conclude that the 3' UTR of the GAPDH mRNA does not appear to possess any structural elements that reduce the efficiency of the progression of XRN1-mediated decay.

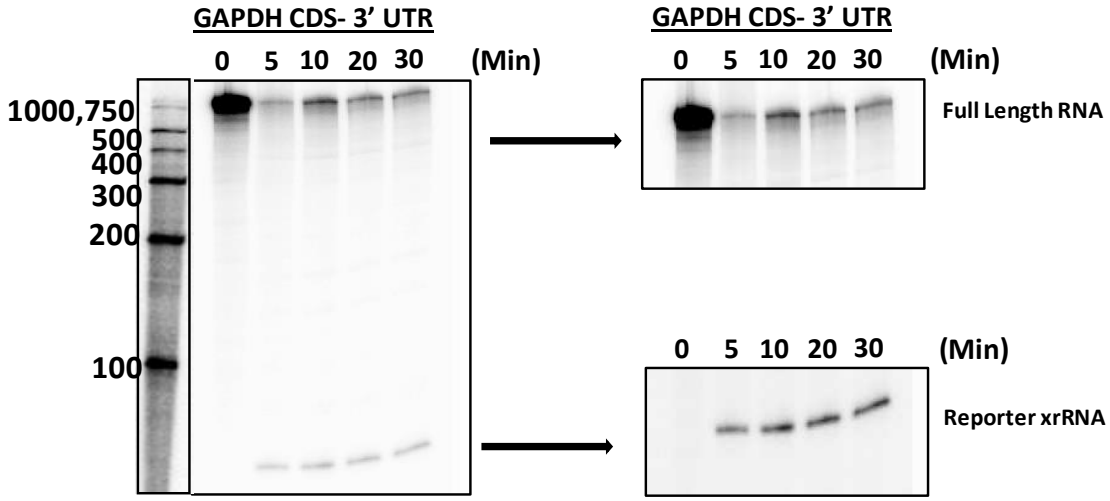

Figure 5. XRN1 decay assay of the GAPDH CDS-3' UTR construct with a time course of 30 minutes. Whole gel image is provided to show the size of RNAs and size of decay intermediate. Upper inset, Zoom to show input RNA decay. Lower inset, zoom to show reporter xrRNA accumulation.

Next, we examined the decay kinetics of the GAPDH CDS-BNYV construct that contains an internal known XRN1 stalling site. As seen in Fig. 6A, the inserted XRN1-stalling structure caused the formation of a clear decay intermediate as expected from previous work[57]. In addition, as seen in the bottom inset of Fig. 6A, the insertion of the BNYV segment clearly slowed the kinetics of the accumulation of the DENV2 xrRNA reporter band compared to the constructs presented in Figs 4 and 5. As seen in the graph in Fig. 4B, the xrRNA reporter readout continued to accumulate throughout the time course rather than achieving an approximate steady state-type level by 10 minutes as seen with the GAPDH-CDS RNA substrate (Fig. 4B). Thus, we

conclude that internal structural elements can indeed stall the progression of XRN1 and that the assay system that we developed will allow the visualization of such internal stalling either by the presence of a novel band on the gel or by the delayed accumulation of the xrRNA reporter readout.

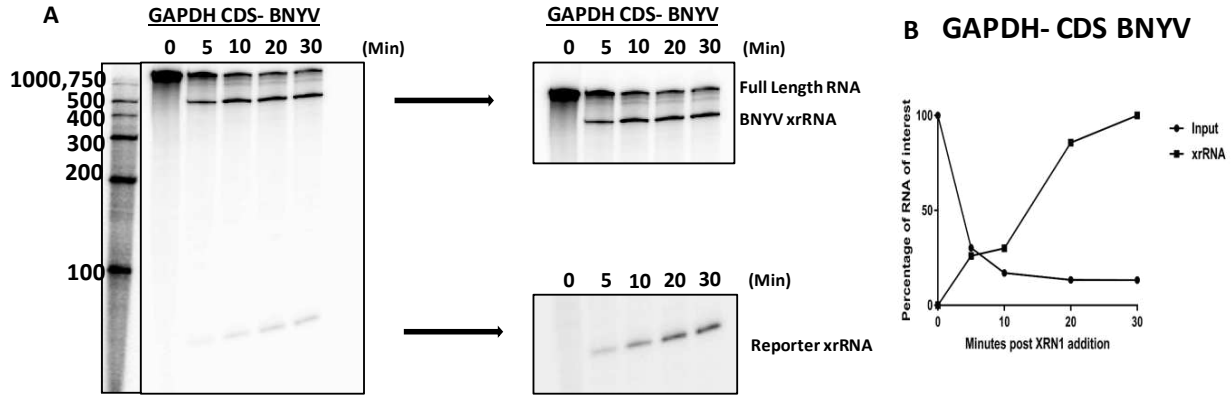

Figure 6. XRN1 decay assay of the Beet Necrotic Yellow Vein (BNYV)-containing construct. The GAPDH CDS-BNYV construct was incubated with XRN1 over a time course of 30 minutes. Panel A. Top inset shows decay of input RNA and the accumulation of the BNYV xrRNA. Bottom inset shows accumulation of reporter xRNA. Panel B. The ratio of percent maximal accumulation over time of either the input RNA or reporter xrRNA.

Finally, we examined the decay kinetics of was the GAPDH-CDS SL RNA which contains an 87 base internalized stem loop structure. As seen in Figure 7 (top inset), the presence of the stem loop stalled XRN1 and resulted in the weak but detectable accumulation of a decay intermediate. This was unexpected as XRN1 was previously thought to be generally able to effectively decay through standard RNA secondary structures. Similar to the situation with the GAPDH CDS-BNYV construct in Fig. 6, the stalling of XRN1 at the internal stem loop structure led to a delay in the kinetics of accumulation of the terminal xrRNA reporter fragment. In summary, these data indicated that the 87nt stem loop structure is a *bona fide* XRN1 stalling

moiety and adds another structure to the growing list of RNA domains that affect the progression of XRN1 on RNA substrates.

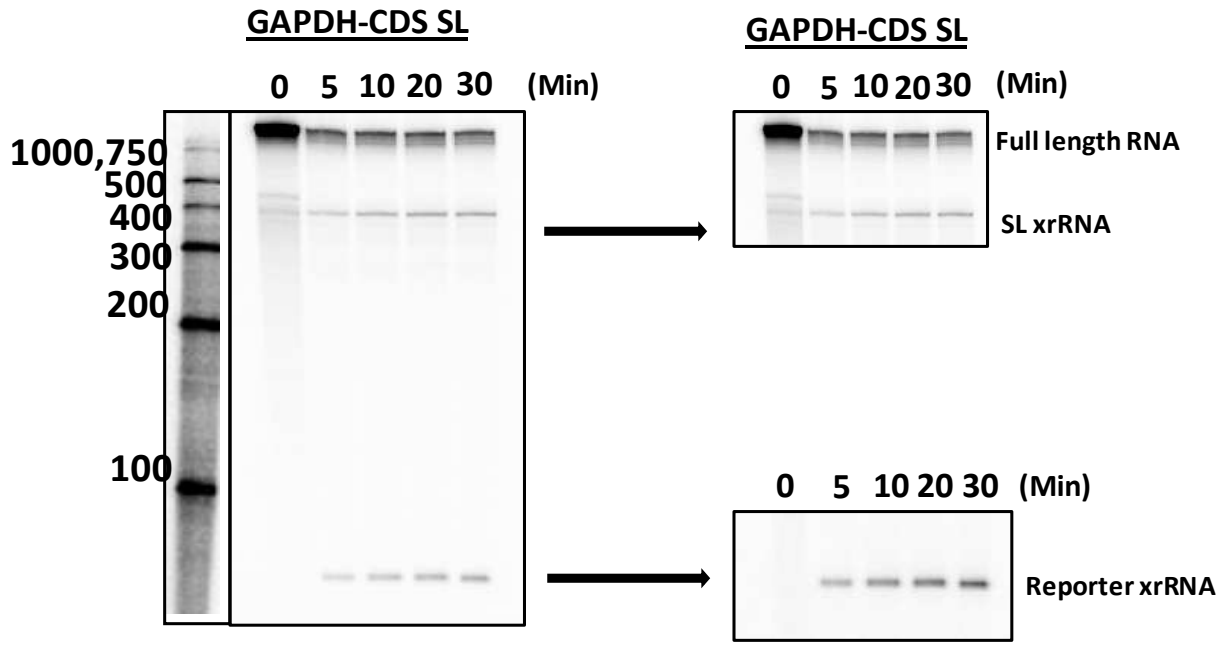

Figure 7. XRN1 Decay assay of the artificial 87 base stem loop-containing construct. The GAPDH-CDS SL RNA substrate was incubated with XRN1 over a time course of 30 minutes. The top inset shows the decay of the input RNA and the accumulation of the stem loop-mediated xrRNA. The bottom inset shows the accumulation of the reporter xRNA.

In conclusion, these data collectively validate the utility of attaching an xrRNA domain to the 3' end of long RNA substrates to allow for an effective evaluation of XRN1 decay kinetics. We believe that this method that can be applied to mRNA-sized substrates, allowing *in vitro* RNA decay assays to be performed with complete, biologically relevant mRNA-type molecules to begin to address questions including combinatorial regulation of mRNA decay and the impact of long range RNA-RNA interactions on decay rates in a controlled, quantifiable system.

Fine mapping of the sequence requirements for the 5' UTRs of Bovine Viral Diarrhea Virus and Hepatitis C Virus genomic RNAs to stall XRN1 and the relationship of XRN1 stalling to internal ribosomal entry sites

The majority of XRN1 stalling sites found to date have been localized to the 3' UTRs of viruses. However, our laboratory has previously demonstrated that there are two viruses that possess XRN1 stall sites in their 5' UTRs - Hepatitis C Virus and Bovine Viral Diarrhea Virus[59] The presence of 5' UTR XRN1 stall sites evokes two key questions. First, what are the minimal sequence elements required for XRN1 stalling at this novel location. The structure may, for example, be very different than the three-helix junction knot present at the 3' UTR of the insect-borne members of the *Flaviviridae*. Second, while XRN1 stalling in the 3' UTRs of viral RNAs creates shorter non-coding RNAs that may function as sponges for a variety of RNA binding proteins[75–77], the function of the large RNA decay intermediate formed by XRN1 stalling in the 5' UTR is unclear. Since the XRN1 stall sites are located upstream of the major structural element that defines the IRES in both HCV and BVDV, we hypothesized that the decay intermediates generated by XRN1 stalling might still be translatable and serve as templates for viral protein production. Addressing these two key questions was the goal of this part of my thesis research.

To map the boundaries of both the BVDV and HCV XRN1 stalling structures, we used a PCR approach to truncate the 5' UTR sequence of each virus by 50nt at a time (Figure 8). As seen in Fig. 9, truncation of 100nt from the 3' end of the 5' UTR of BVDV was sufficient to eliminate the production of the decay intermediate marked 2. The decay intermediate labeled 1 was generated until the BVDV 5' UTR sequence was truncated down to 140 nucleotides (Fig. 8E). In summary, 3' deletion analysis of the 5' UTR of BVDV illustrates two key points with

regard to XRN1 stalling. First, as seen in the secondary structure diagram in Fig. 8, the BVDV #1 XRN1 stall site appears to require a single stem loop structure based on the canonical secondary structure model of the 5' UTR. This is reminiscent of the data that we obtained with the extended stem loop structure in the GAPDH-CDS SL RNA construct during our method development work seen in Fig. 7. Second, BVDV XRN1 still site #2, on the other hand, appears to require the majority of the extended structural moiety of the IRES. This raises the possibility that IRES elements in general may be difficult for XRN1 to navigate through.

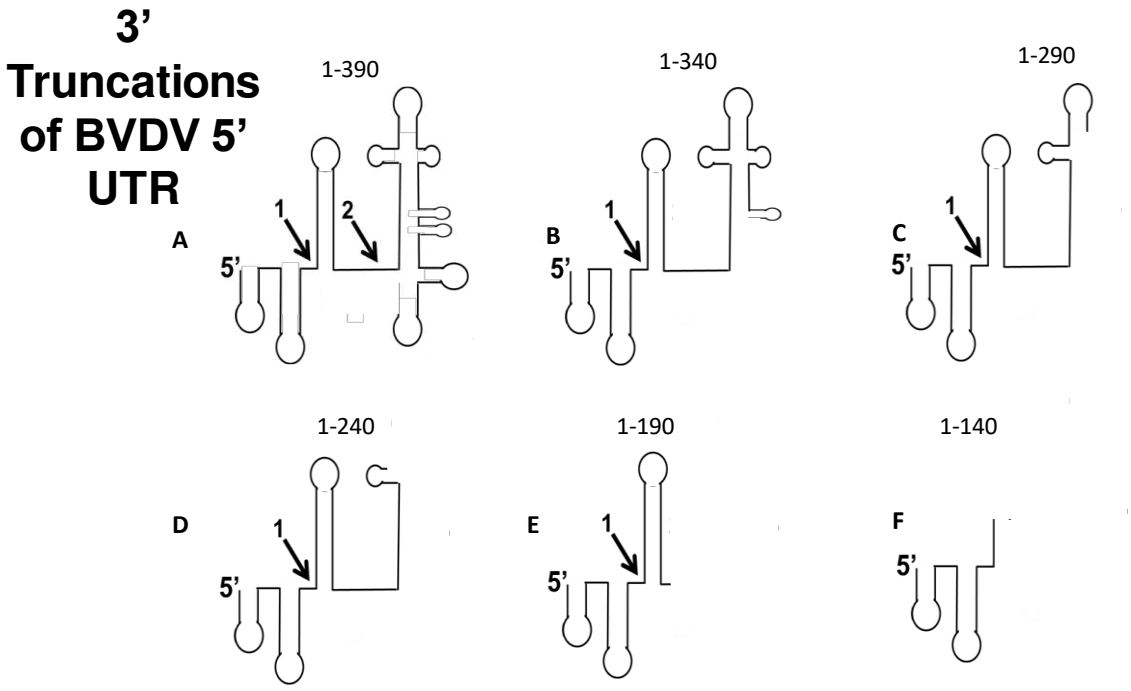

Figure 8. Schematic of 3' truncation mutants generated in the 5' UTR of BVDV

The numbers represent XRN1 stall sites that have been previously described. Based on the data in Fig. 6, when the production of a decay intermediate by XRN1 stalling is disrupted in a truncated RNA substrate, the number is removed from the schematic.

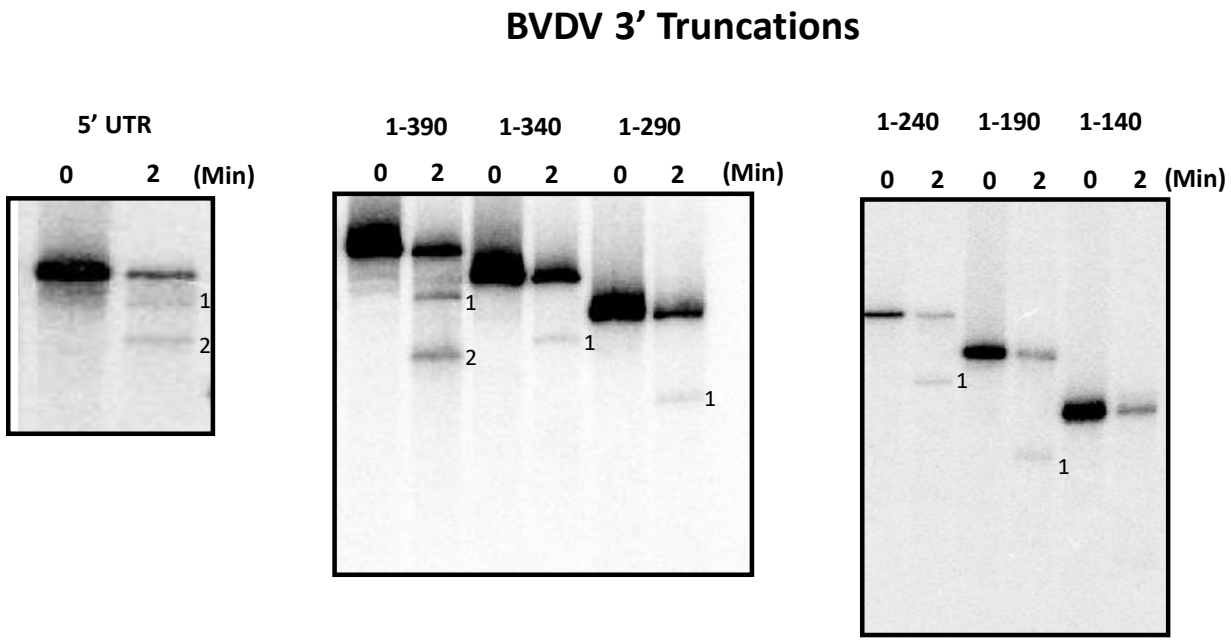

Figure 9. XRN1 decay assays of RNA substrates containing progressive 3' truncations of the BVDV 5' UTR

Left Panel. Representative decay assay of the entire BVDV 5' UTR. XRN1 decay intermediates are labelled 1 and 2

Middle Panel. XRN1 decay assay of truncated RNA substrates 1-390. 1-340, and 1-290 (as diagrammed in Fig. 5). Note that decay intermediate 2 disappears after 100nt were deleted (see RNA substrate 1-340).

Right Panel. XRN1 decay assay of truncated RNA substrates 1-240. 1-190, and 1-140 (as diagrammed in Fig. 5). Note that decay intermediate 1 disappears after 300nt were truncated in construct 1-140.

IRES element mediated XRN1 stalling does not appear to be omnipresent amongst viruses with IRES elements.

As the 5' UTR stalling of XRN1 on BVDV and HCV RNAs appears to be a unique mechanism amongst flaviviruses, we wanted to investigate the ability of other IRES elements to stall XRN1. To do this we examined an RNA substrate containing the poliovirus IRES element along with a DENV2 xrRNA structure near its 3' terminus in our modified XRN1 decay assay as outlined in Figs 4-7. As can be seen in Figure 10, there does not appear to be any novel XRN1 decay intermediates formed from the poliovirus IRES region of the RNA substrate. The

presence of the background RNA decay from contaminating ribonuclease does, however, leave open the possibility of weak XRN1 stalling may be occurring. Thus, we conclude that the induction of strong, efficient XRN1 stalling is not necessarily a feature of all IRES elements.

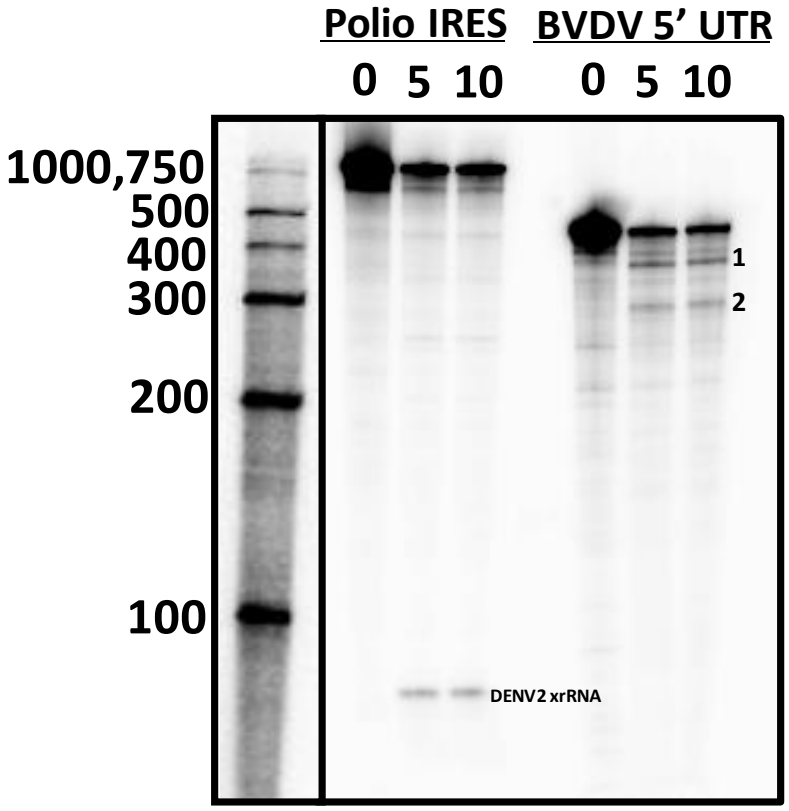

Figure 10. RNA decay intermediates do not accumulate to substantial levels in an XRN1 decay assay of an RNA substrate containing the Poliovirus 5' UTR.
5' monophosphorylated RNAs containing the poliovirus 5' UTR (Polio IRES) or the BVDV 5' UTR (BVDV 5' UTR lanes) were incubated with XRN1 for the times indicated. Reaction products were analyzed on a 5% acrylamide gel.

The 5' UTR truncated XRN1 RNA decay intermediates of both HCV and BVDV retain the ability to act as functional translation templates *in vitro*.

Finally, we sought to investigate the potential that the XRN1 decay intermediates generated from the 5' UTRs of BVDV and HCV might preserve the ability to be translated through IRES-driven translation. This would provide a biological function for the accumulated

decay intermediates in viral infections. To test this hypothesis, we devised a series of RNA constructs to be used in *in vitro* translation assays. As a positive control, we inserted the 5' UTRs of HCV and BVDV upstream of the GFP open reading frame through a Gibson assembly approach. Both capped and uncapped RNA transcripts were generated and used in a Rabbit Reticulocyte (RRL) *in vitro* translation assay to assess the accumulation of GFP protein. As uncapped RNAs can only initiate translation through the use of the IRES element, the uncapped RNAs allowed for a definitive assessment of IRES function. Figure 11 shows the basic design premise of these constructs. After RRL translation, we performed an immunoprecipitation using GFP antibodies and western blotting to cleanly assess protein production from the RNAs we included in the assay.

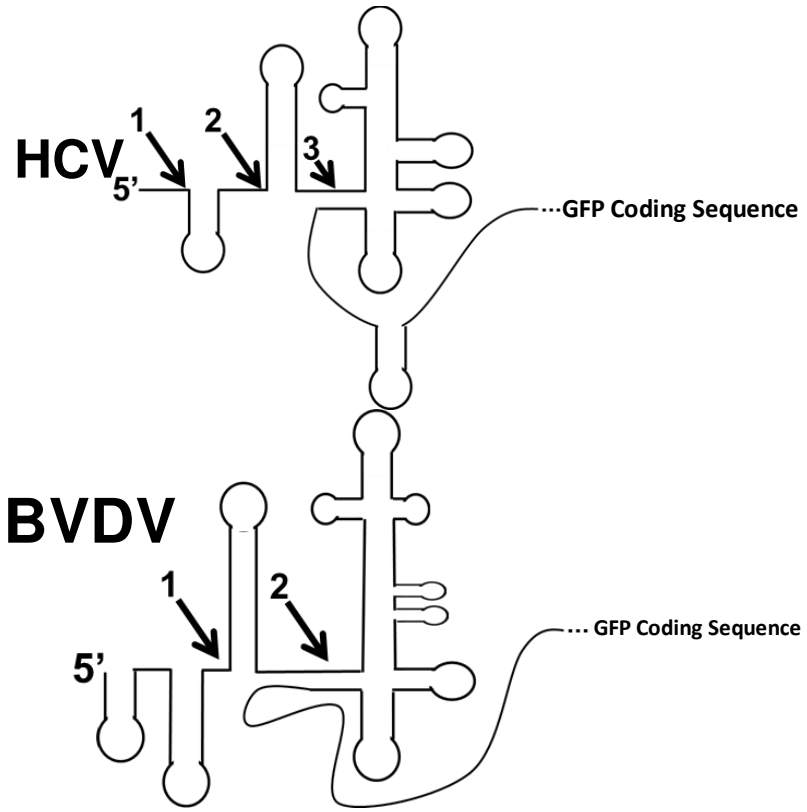

Figure 11. Design of constructs to assess IRES-mediated translation of 5' UTR XRN1 decay intermediates
The numbers refer to sites of XRN1 stalling as determined previously

As seen in Figure 12A, both the uncapped and capped RNAs produced a protein of approximately the correct size (27kDa) for GFP in the HCV 5' UTR construct. Similar results were obtained for the full length BVDV 5' UTR (Fig. 12B). To investigate whether or not the stable XRN1 decay intermediates generated from both viral 5' UTRs retained IRES function, we prepared GFP encoding RNAs that contained the respective viral 5' UTRs starting at the indicated XRN1 stall sites rather than the 5' end of the viral genomic RNA. As seen in Figure 13, RNAs starting at either the 2nd or 3rd XRN1 stall site of the HCV 5' UTR (representing the major XRN1 decay intermediate of the virus) retained at least partial IRES function as seen by their ability to generate the ~27kDa GFP protein as seen with the full length or capped constructs. The anomalous ~18kDa band observed in all of our RRL is likely either due to non-specific antibody binding or represents a proteolytic degradation product of GFP. Interestingly, RNAs representative of the shortest decay intermediate of HCV (Fig. 13C) also retained translatability, indicating that the function of all of the XRN1 decay intermediates generated from the HCV 5' UTR may be to serve as functional mRNAs for translation. As seen in Fig. 14, both of the XRN1 decay intermediates of BVDV also retained the ability to translate the GFP open reading frame. Taken together these results indicate that the function of XRN1 decay intermediates generated from the 5' UTR of non-insect borne members of the *Flaviviridae* may be to serve exclusively as functional mRNAs to generate viral proteins to promote viral growth and replication.

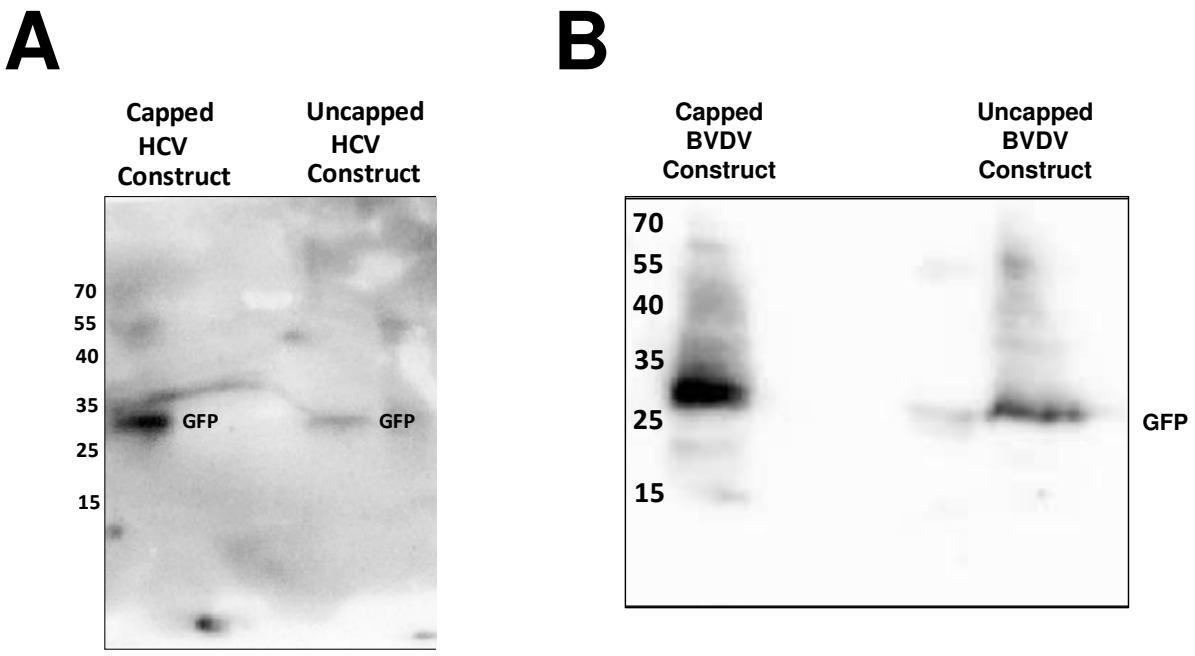

Figure 12. The HCV and BVDV 5' UTRs contain functional IRES elements
The indicated RNAs were incubated with rabbit reticulocyte lysate. Translation products were concentrated using anti-GFP antibodies and the 27 KDa GFP produced by in vitro translation was detected by western blotting.

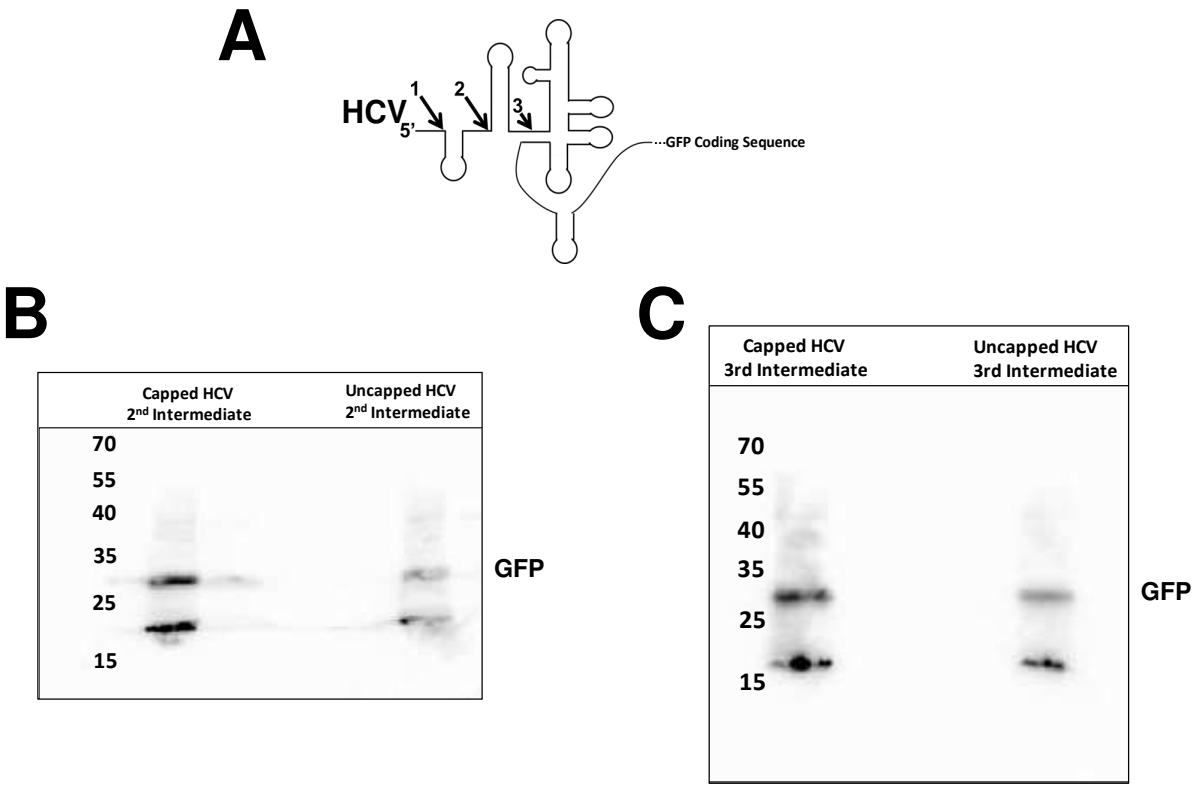

Figure 13. The HCV 5' UTR XRN1 decay intermediates retain functional IRES elements

The indicated RNAs were incubated with rabbit reticulocyte lysate. Translation products were concentrated using anti-GFP antibodies and the 27 KDa GFP produced by in vitro translation was detected by western blotting. The identity of the ~18 KDa band in the assay is unclear. It may represent a GFP proteolytic fragment or a non-specific band detected by the antibody.

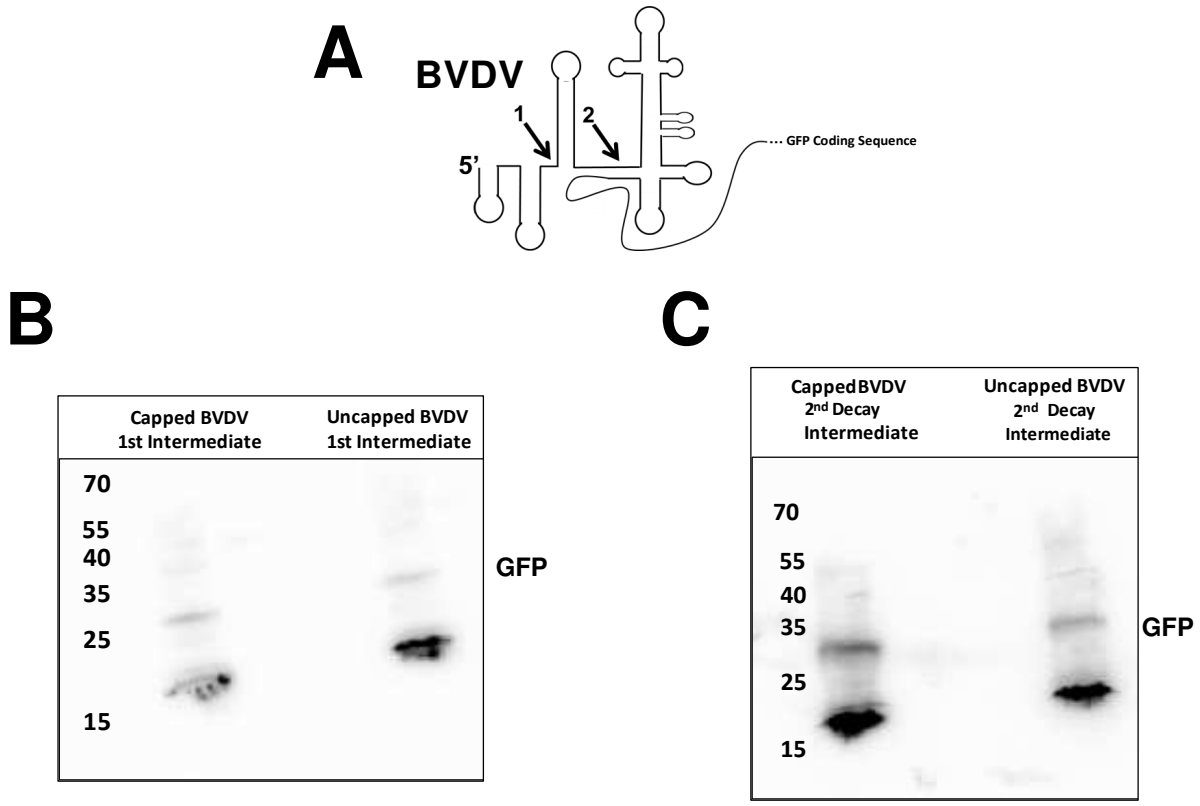

Figure 14. The BVDV 5' UTR XRN1 decay intermediates retain functional IRES elements

The indicated RNAs were incubated with rabbit reticulocyte lysate. Translation products were concentrated using anti-GFP antibodies and the 27 KDa GFP produced by in vitro translation was detected by western blotting. The identity of the ~18 KDa band in the assay is unclear. It may represent a GFP proteolytic fragment or a non-specific band detected by the antibody

Discussion

Engineered Viral Decay Intermediates to Assess XRN1-mediated Decay.

The overarching idea of this study was to find a way to circumvent a critical weakness present in the decay assays utilized in previous studies by this lab and others, that of the resolution power of denaturing PAGE. While RNA fragments that are relatively small, up to 400 bases[78,79], dependent on polyacrylamide percentage- separate in a manner that is easily visualized, with larger fragments it becomes nigh impossible to see separation between decay products and input RNA bands. Previously our lab and others have focused on the utilization of fragmented sections of mRNAs, 3' UTRs, 5' UTRs or fragments of the coding sequence (CDS) that do not possess all of the elements/structures that may play a role in the combinatorial regulation of the decay of the transcript. As accurate *in vitro* reconstitution of biological systems is essential to truly understanding to the effective use of this approach to determine what is occurring over the course of viral infection, we sought to increase the effectiveness of our *in vitro* decay assays. We hypothesized that we could utilize a decay intermediate formed by the DENV2 XRN1 resistant RNA (xrRNA) as a readout to allow for observation of decay of large RNAs. In addition, this assay allows for improvements in the approach to understanding XRN1 decay kinetics brought about by structural elements within the RNA being decayed.

The first RNA interrogated in this modified assay was the control sequence composed of the GAPDH open reading frame, an RNA that was presumed to lack xrRNA activity. As expected, we were able to observe rapid degradation of the input RNA and accumulation of the xrRNA readout (Fig 4). This control established that our hypothesis of utilizing the DENV2 xrRNA as a readout for an RNA larger than 400nt was viable and allows for observation of a

resolvable decay intermediate from the parent RNA substrate. In addition, measurement of the ratio of decay to accumulation of the xrRNA intermediate allowed us to more effectively quantify the decay kinetics of XRN1. The establishment of a decay profile in this control RNA is what allowed us to interrogate change in decay rates of our further constructs.

Due to the propensity for xrRNAs to exist in the 3' UTR of viral transcripts[51–53,57,80,81], we wanted to investigate the possibility that 3' UTRs of cellular mRNAs exhibit an inherently slower decay profile due to their proclivity to be more structured[74] than their coding sequence counterparts. To affect this, we created a construct that possessed the 3' UTR of GAPDH. As can be seen in Figure 5, the decay profile of this transcript was very similar to that of the control GAPDH-CDS substrate. This does not, of course, preclude the possibility that other cellular 3' UTRS might exhibit more xrRNA activity than CDS sequences.

The structure intended to alter the decay profile of our constructs was created utilizing an xrRNA from a different virus family (*Benyviridae*) than DENV2. By inserting a known XRN1 stalling structure into the GAPDH-CDS RNA substrate, we hoped to observe a change in the decay profile, either visualizing a lack of accumulation of the readout DENV2 xrRNA due to complete stalling on the Beet Necrotic Yellow Vein xrRNA, or a slowed rate of accumulation of our readout xrRNA. As can be seen in Fig. 6, while the decay of the input RNA proceeds at a rapid pace comparable to the control GAPDH-CDS RNA, the accumulation of the xrRNA is indeed slower. This lack of 1:1 molar accumulation of input to readout suggests that there is a potential pliability of the BNNYV xrRNA that allows XRN1 to slowly "break-through" the xrRNA and allow for further degradation of the RNA. This observation is supported by previous work in our lab that indicates that both Hepatitis C Virus and Bovine Viral Diarrhea Virus, as well as many of the insect-borne flaviviruses, possess multiple sequential XRN1 stalling sites[59].

Importantly, in order to accurately assess changes in decay profiles of other RNAs, this ability of the XRN1 stalling structure to quantitatively interfere with XRN1 must be considered.

Finally, the work described above also adds a new structure capable of stalling XRN1 to the molecular biology toolbox. This 87nt stem loop structure can be utilized in a variety of ways including investigation of which RNA decay pathway RNAs are shuttled down in mammalian decay. The methodology utilized in yeast for this, a poly(G) tract[82], is not particularly effective in mammalian cells[83], and as such the discovery of a new tool to interfere with XRN1 activity could lead to discoveries in this area.

Overall, we have demonstrated the power of this method for utilization as a readout for decay of larger RNAs. We have also demonstrated that measurement of the accumulation of the xrRNA readout can be used in a limited capacity for examination of the decay kinetics of XRN1 substrates. We have also shown evidence that contributes to the theory that xrRNA structures are not immutable but instead maintain a level of pliability that XRN1 is able to exploit to degrade RNA. This method allows us to add yet another assay to the list of tools that utilize xrRNA structures as readouts for measurements of decay. As seen in both the development of the xrFrag[73] and the TREAT methods[71,72], xrRNA structures continue to represent powerful tools in the examination of decay modulation with single target molecules. The ability to examine single molecule populations rather than make conclusions about single mRNAs off of a population dynamic, allows for more accurate estimations of mRNA lifecycles to be made.

Examination of sequence requirements for xrRNA activity in BVDV reveals two regions of interest.

The majority of XRN1-resistant RNAs to date have been localized to the 3' UTR of various viruses[52,53,57]. Our lab, however, has previously demonstrated the ability of two viruses, Hepatitis C virus and Bovine Viral Diarrhea virus, to stall XRN1 at their 5' ends[59]. Due to the novel properties of 5' stall sites, we sought to investigate two areas. One, we wanted to elucidate the minimal sequence requirements necessary to stall XRN1 at these locations. Structural difference between the well described flavivirus 3' UTR stalling structures and the structures present in the 5' UTRs of these viruses is very possible and thus identifying a minimal stalling structure represents foundational data for future structural investigations in this area. Second, while the 3' UTR stalling sites have the potential to act as sponges for several RNA binding proteins and interfere with XRN1 activity[75,77,84], the biological purpose of these 5' UTR sites (aside from stalling XRN1) is currently unknown. As the XRN1 stall sites are located upstream of the core structural elements that define the IRES elements in both BVDV and HCV, we hypothesized that the decay intermediates generated by XRN1 stalling in these viruses might still possess the capability to be translated and thus generate viral proteins.

The first step in this process was to examine the boundaries of the BVDV stalling structures. We utilized a PCR approach to generate progressive 50nt truncations of the 5' UTR as diagrammed in Fig. 8. The decay intermediate labelled 1 required truncation of the 5' UTR down to 140 nucleotides before its production was eliminated. Examination of the canonical BVDV 5' UTR reveals a stem loop structure that matches up with the XRN1 stall location in BVDV. These data are reminiscent with what was observed with the GAPDH-CDS Stem Loop construct utilized in our method development work seen in Fig. 7. This observation could help

lead down the road to predictive identification of other XRN1 stall sites in currently uninvestigated viral or cellular RNAs. As seen in Figure 9, truncation of 100nt was sufficient to eliminate the production of the decay intermediate marked 2. A 100nt truncation appears to eliminate several domains that are critical to proper formation of the IRES elements[61,85,86] in both HCV and BVDV. These data suggest that proper IRES element folding is required to establish a second xrRNA structure in BVDV. Both HCV and BVDV possess a series of nucleotide interactions upstream of the AUG that form a pseudoknot that contributes to translation efficiency. In BVDV this interaction occurs approximately 20 nucleotides upstream of the AUG with a series of nucleotides approximately 80 nucleotides upstream of the AUG[86]. HCV possess a similar series of interactions between nucleotides 126-134 and nucleotides 315-323 forming one stem loop of the pseudoknot, and nucleotides 305-311 bind with nucleotides 325-331 forming the second stem loop of the pseudoknot[85]. Taken together the existence of these pseudoknot structures implies that the 3' end of the viral IRES elements are perhaps the most essential structural elements to viral translation efficiency. Examination of the 5' stall sites through this lens reveals that the stalling of XRN1 protects both the full length IRES and protects the critical pseudoknots function necessary for efficient translation. Additionally, the possibility of all IRES elements possessing some level of xrRNA activity is raised by this data.

IRES element mediated XRN1 stalling does not appear to be a conserved mechanism amongst viruses.

BVDV and HCV are not unique in their possession of IRES elements, in fact a wide variety of viruses utilize an IRES element to initiate translation. Amongst those viruses is poliovirus, a member of the *Picornaviridae.* BVDV and HCV are, however, unique amongst their family members for the presence of 5' UTR XRN1 stall sites. Due to the fact that our

mapping of BVDV revealed that the entire IRES is necessary for stalling, we wanted to investigate if other IERS elements possess XRN1 stalling activity. To investigate this, we utilized the method outline in Figures 4-7 to allow for examination of the entire poliovirus IRES at once with the ability to resolve decay intermediates as the poliovirus IRES sequence is ~910 nucleotides in length and it would thus be difficult to resolve decay intermediates from the parent RNA substrates. We attached the DENV2 XRN1 stalling sequence on the end of the poliovirus IRES sequence in a similar manner to our previously described method. Figure 10 shows that there does not appear to be any novel XRN1 decay intermediates formed. However due to background degradation from a contaminating ribonuclease, there remains the possibility that some weak XRN1 stalling might be occurring that are masked by this degradation. We do conclude from this Figure, however, that strong XRN1 stalling is not necessarily a feature of all IRES elements. Further investigation into this area would involve other viruses with IRES elements such as encephalomyocarditis virus (EMCV), or in cellular mRNAs[87].

IRES elements exist within the 5' UTRs of viruses that cannot or do not undergo canonical translation in an infected cell. The elements act to recruit necessary factors to allow for the viral transcript to undergo translation. Interestingly, not all IRESs function in the same manner. There are in fact four types of viral IRES elements currently characterized, some more so than others, that differ in what translation factors they recruit and what structural elements are required[60]. These elements are so titled the Group 1-4 IRES elements.

Group 1 IRES elements bind to the ribosome directly without need of Met-tRNA$_i$ or translation protein factors. These IRES elements are located in the family of *Dicistroviridae* of the *Picornaviridae* that affect invertebrate insects[88]. Of particular interest with this group of IRES elements is the bicistronic nature of their translation initiation. Group 1 IRES viruses

possess two IRES elements, one located in their 5' UTR, and one located in the intergenic region (IGR), which is located between the two ORFs [88]. The IRES elements these viruses possess are unique with regards to the fact that they do not initiate translation at an AUG, instead utilizing a non-AUG start codon[88]. These viruses also initiate translation in the ribosomal A-site rather than the P-site. Lastly, these viruses do not require any of the canonical translation initiation factors[88]. The structural elements of the Group 1 IRES possess a complicated secondary and tertiary structure made up of three pseudoknots and two conserved stem loops that act to make direct contact with the 40S subunit[89,90]. These elements form a unique, tightly folded globular structure that allows for pre-positioning of the ribosome interacting elements of the IRES[91]. These tightly folded structures are of interest as they have the potential for possessing xrRNA activity. However due to the possession of a VPg at their 5' end, it is possible that these viruses are not prime targets for 5'-3' XRN1-mediated degradation[92].

Group 2 IRES elements adopt wildly different structural elements to the IGR IRES elements and do not possess the same tight globular structure folding present in the IGR IRES elements[93,94]. Instead, viruses with these Group 2 elements, such as HCV, BVDV, and Classical Swine Fever virus, possess lengthy IRES sequences that possess multiple conserved stem loops. The stem loops located in these IRES elements act in making direct contact to the ribosome and associated translation factors EIF2 and EIF3[66]. Due to the conserved nature of these stem loops, these stem loop elements likely contribute to the xrRNA activity of the BVDV IRES elements. In addition, as these viruses lack a poly(A) tail and 7mG cap, they are prime targets for XRN1-mediated decay.

Group 3 and Group 4 IRES elements do not have in-depth structural analysis akin to those performed on the Group 1 and 2 elements. However, information regarding their

recruitment of translation factors is relatively well studied. Group 3 elements, which are possessed by viruses like EMCV , Foot-and-Mouth Disease Virus (FMDV), and Theiler's murine encephalomyelitis virus (TMEV)[64,95,96], require binding of EIF4A, 4B, 4G, EIF3, EIF2, and some number of IRES trans-activating factors in a presumably structurally dependent manner[60]. While the structural nature of translation initiation within these IRES elements has not been elucidated, there are sequence regions of interest that would be an excellent avenue for structural investigation[64,95,96]. The Group 4 IRES elements, possessed by poliovirus and Rhinoviruses, also lack intensive structural analysis, but do require a similar suite of translation factors as seen in Group 3 IRES elements[65,97]. Similar to the Group 3 IRES elements regions of interest in these viruses have been identified and utilized for initiation of translation and thus could be used for investigation of xrRNA activity. However due to the mRNA of both poliovirus and EMCV, along with other picornaviruses, containing VPg covalently attached to their 5' end and possession of a poly(A) tail[65,96], these viruses once again may not be targeted for 5'-3' degradation.

As the IRES elements present in HCV and BVDV are both Group 2 elements, it is possible that the inhibition of XRN1 is a conserved function amongst this group of IRES elements rather than a conserved feature of IRES elements in general. The lack of a strong stalling sequence present in the poliovirus IRES element, a member of the Group 4 IRES elements, suggests this. Future studies in this area should focus on examining further members of each IRES group, Group 3 IRES: EMCV, Foot and Mouth Disease virus; Group 4 IRES: poliovirus, and rhinoviruses; Group 1 IRES: Cricket Paralysis Virus, Taura Syndrome Virus, or further examination of the other Group 2 IRES elements such as those found in Classical Swine Fever Virus and Porcine Teschovirus 1[62–65,96–100]. If further stall sites are located in Group 1,3, or

4 IRES element possessing viruses, viral infection should be evaluated in the context of XRN1 knockdown cells to establish that XRN1 plays a role in the decay of these viruses. This secondary analysis is necessary due to the potential of these viral RNAs to evade decay due to their poly(A) tail or the possession of the VPg protein.

The 5' UTR truncated XRN1 RNA decay intermediates of both HCV and BVDV retain the ability to act as functional translation templates *in vitro*.

The final area we wanted to investigate was the potential for the 5' decay intermediates of HCV and BVDV to retain their ability to undergo IRES mediated translation. If this were the case it would confirm our hypotheses and the mounting evidence that the major biological purpose of these stall sites is to protect the IRES element and the message all in one, allowing for a translational-based strategy rather than the more common XRN1 activity inhibition[55,77]. As demonstrated by Figures 12, 13 and 14 the constructs display a continued ability to act as a viable translation template even with the 5' UTR truncated at XRN1 stalling sites. This lends credence to our hypothesis that the biological function of these 5' stalling elements is to preserve the message of the RNA and act as a translation template.

One potentially interesting interplay with the decay intermediates of BVDV and HCV might be that of the ability of the virus to generate a subpopulation of RNA that is specifically to be translated rather than packaged. Current evidence shows that while the 5' UTR aids in the efficiency of the production of trans-complemented HCV particles, deletion of the 5' UTR does not prevent their formation as deletion of the 3' UTR does[101,102]. This suggests that the 5' UTR is not essential to viral packaging and therefore its partial decay could act as a way to mediate the virus' decision making as to which transcripts to package and which transcripts to utilize for translation.

Another aspect that could be mediated by the partial decay of HCV mRNAs is that of the sequestering of miR-122. MirR-122 binds in two locations on the HCV 5' UTR and acts to positively affect the translation of the viral replication[103,104]. Interestingly, miR-122 binding has no effect on the translation of viral proteins. This once again plays into the possibility that partially decayed HCV transcripts are not utilized for replication of the virus, but instead act as translation templates allowing the virus to focus its efforts on the generation of packaged viruses.

Further research in this area should be focused on the creation of full HCV or BVDV RNAs with 5' UTRs representative of the partial decay by XRN1 and the ability of the virus to replicate and produce viral particles examined This focus could allow for the teasing out of roles of partially decayed UTRs with regards to a shuttling of viral transcripts towards translation vs packaging. Being able to track the ultimate fate of partially decayed RNAs through the translation and packaging process utilizing a method such as TREAT[72] could lend credence to the idea of sub-populations of RNAs being utilized as translational templates rather than existing as a packageable viral genome.

Overall, the data presented herein is an excellent first step on the road to understanding the unique 5' UTR structures that BVDV and HCV possess. It also reveals the potential for other 5' UTR stalling elements to exist in viruses that possess similar IRES elements to HCV and BVDV. This point merits further investigation. The modified decay assay method presented herein represents a perfect opportunity to allow for investigation of the other Group II IRES elements in full biological context.

References

1. Medscape Commentary, Dr. Tyler Sharp, C. Dengue | CDC. Centers for Disease Control and Prevention (2016).

2. Scherwitzl, I., Mongkolsapaja, J. & Screaton, G. Recent advances in human flavivirus vaccines. Current Opinion in Virology (2017). doi: 10.1016/j.coviro.2017.04.002

3. Vos, T., Allen, C., Anora, M., Brown, A., Carter, A., et al. Global, regional, and national incidence, prevalence, and years lived with disability for 310 diseases and injuries, 1990–2015: a systematic analysis for the Global Burden of Disease Study 2015. Lancet (2016). doi:10.1016/S0140-6736(16)31678-6

4. Kish, T., Aziz, A. & Sorio, M. Hepatitis C in a new era: a review of current therapies. P&T 42, 316–329 (2017).

5. Moennig, V., Houe, H. & Lindberg, A. BVD control in Europe: current status and perspectives. Anim. Heal. Res. Rev. (2005). doi:10.1079/ahr2005102

6. Lindberg, A., Brownlie, J., Gunn, G.J., Houe, H., et al. The control of bovine viral diarrhoea virus in Europe: today and in the future. Revue scientifique et technique (International Office of Epizootics) 25, 961–79 (2006).

7. Nickell, J. S., White, B. J., Larson, R. L., Renter, D. G. & Sanderson, M. W. A simulation model to quantify the value of implementing whole-herd bovine viral diarrhea virus testing strategies in beef cow-calf herds. J. Vet. Diagnostic Investig. (2011). doi:10.1177/104063871102300202

8. Schoenberg, D. R. & Maquat, L. E. Regulation of cytoplasmic mRNA decay. Nature Reviews Genetics (2012). doi:10.1038/nrg3160

9. Garneau, N. L., Wilusz, J. & Wilusz, C. J. The highways and byways of mRNA decay. Nature Reviews Molecular Cell Biology (2007). doi:10.1038/nrm2104

10. Lykke-Andersen, S. & Jensen, T. H. Nonsense-mediated mRNA decay: An intricate machinery that shapes transcriptomes. Nature Reviews Molecular Cell Biology (2015). doi:10.1038/nrm4063

11. Yang, F., Peng, Yong., Murray, E., Otsuka, Y., et al. Polysome-Bound Endonuclease PMR1 Is Targeted to Stress Granules via Stress-Specific Binding to TIA-1. Mol. Cell. Biol. (2006). doi:10.1128/MCB.00090-06

12. Chernokalskaya, E., Dubell, A.N., Cunnigham, K.S., Hanson, M.N., et al. A polysomal ribonuclease involved in the destabilization of albumin mRNA is a novel member of the peroxidase gene family. RNA (1998). doi:10.1017/S1355838298980451

13. Yang, F. & Schoenberg, D. R. Endonuclease-mediated mRNA decay involves the selective targeting of PMR1 to polyribosome-bound substrate mRNA. Mol. Cell (2004). doi: 10.1016/j.molcel.2004.05.001

14. Hollien, J. & Weissman, J. S. Decay of endoplasmic reticulum-localized mRNAs during the unfolded protein response. Science (104-107) (2006). doi:10.1126/science.1129631

15. Xiao, S., Scott, F., Fierke, C. A. & Engelke, D. R. Eukaryotic Ribonuclease P: A Plurality of Ribonucleoprotein Enzymes. Annu. Rev. Biochem. (2002). doi: 10.1146/annurev.biochem.71.110601.135352

16. Schmitt, M. E., Cai, T., Aulds, J., Wierzbicki, S. & Gill, T. RNase MRP Cleaves the CLB2 mRNA To Promote Cell Cycle Progression: Novel Method of mRNA Degradation. Mol. Cell. Biol. (2004). doi:10.1128/mcb.24.3.945-953.2004

17. Liu, J., Carmell, M.A., Rivas, F.V., Marsden, C.J., et al. Argonaute2 is the catalytic engine of mammalian RNAi. Science Vol. 305 Issue 5689 (1437-1441). (2004). doi:10.1126/science.1102513

18. Song, J. J., Smith, S. K., Hannon, G. J. & Joshua-Tor, L. Crystal structure of argonaute and its implications for RISC slicer activity. Science (1434-1437). (2004). doi:10.1126/science.1102514

19. Frischmeyer, P. A., van Hoof, A., O'Donnell, K., Gurerrio, A.L., et al. An mRNA surveillance mechanism that eliminates transcripts lacking termination codons. Science (2258-2261). (2002). doi:10.1126/science.1067338

20. Van Hoof, A., Frischmeyer, P. A., Dietz, H. C. & Parker, R. Exosome-mediated recognition and degradation of mRNAs lacking a termination codon. Science (2262-2264). (2002). doi:10.1126/science.1067272

21. Inada, T. & Aiba, H. Translation of aberrant mRNAs lacking a termination codon or with a shortened 3′-UTR is repressed after initiation in yeast. EMBO J. (2005). doi: 10.1038/sj.emboj.7600636

22. Schweingruber, C., Rufener, S. C., Zünd, D., Yamashita, A. & Mühlemann, O. Nonsense-mediated mRNA decay - Mechanisms of substrate mRNA recognition and degradation in mammalian cells. Biochimica et Biophysica Acta - Gene Regulatory Mechanisms (2013). doi: 10.1016/j.bbagrm.2013.02.005

23. Kervestin, S. & Jacobson, A. NMD: A multifaceted response to premature translational termination. Nature Reviews Molecular Cell Biology (2012). doi:10.1038/nrm3454

24. Ivanov, P. V., Gehring, N. H., Kunz, J. B., Hentze, M. W. & Kulozik, A. E. Interactions between UPF1, eRFs, PABP and the exon junction complex suggest an integrated model for mammalian NMD pathways. EMBO J. (2008). doi:10.1038/emboj.2008.17

25. Singh, G., Rebbapragada, I. & Lykke-Andersen, J. A competition between stimulators and antagonists of Upf complex recruitment governs human nonsense-mediated mRNA decay. PLoS Biol. (2008). doi: 10.1371/journal.pbio.0060111

26. Cumberworth, S. L., Clark, J. J., Kohl, A. & Donald, C. L. Inhibition of type I interferon induction and signaling by mosquito-borne flaviviruses. Cell. Microbiol. 19, e12737 (2017). doi:10.1111/cmi.12737

27. Joncourt, R., Eberle, A. B., Rufener, S. C. & Mühlemann, O. Eukaryotic initiation factor 4G suppresses nonsense-mediated mRNA decay by two genetically separable mechanisms. PLoS One (2014). doi: 10.1371/journal.pone.0104391

28. Kashima, I., Yamashita A., Izumi, N., Kataoka, N., et al. Binding of a novel SMG-1-Upf1-eRF1-eRF3 complex (SURF) to the exon junction complex triggers Upf1 phosphorylation and nonsense-mediated mRNA decay. Genes Dev. (2006). doi:10.1101/gad.1389006

29. Melero, R., Uchiyama, A., Castano, R., Kataoka, N., et al. Structures of SMG1-UPFs complexes: SMG1 contributes to regulate UPF2-dependent activation of UPF1 in NMD. Structure (2014). doi: 10.1016/j.str.2014.05.015

30. Hug, N. & Cáceres, J. F. The RNA Helicase DHX34 Activates NMD by promoting a transition from the surveillance to the decay-inducing complex. Cell Rep. (2014). doi: 10.1016/j.celrep.2014.08.020

31. Unterholzner, L. & Izaurralde, E. SMG7 acts as a molecular link between mRNA surveillance and mRNA decay. Mol. Cell (2004). doi: 10.1016/j.molcel.2004.10.013

32. Yamashita, A., Chang, T.C., Yamashita, Y., Zhu, W., et al. Concerted action of poly(A) nucleases and decapping enzyme in mammalian mRNA turnover. Nat. Struct. Mol. Biol. (2005). doi:10.1038/nsmb1016

33. Nagarajan, V. K., Jones, C. I., Newbury, S. F. & Green, P. J. XRN 5'→3' exoribonucleases: Structure, mechanisms and functions. Biochimica et Biophysica Acta - Gene Regulatory Mechanisms (2013). doi: 10.1016/j.bbagrm.2013.03.005

34. Huarte, J., Stutz, A., O'Connell, M.L., Gubler, P., et al. Transient translational silencing by reversible mRNA deadenylation. Cell (1992). doi:10.1016/0092-8674(92)90620-R

35. Brown, C. E., Tarun, S. Z., Boeck, R. & Sachs, A. B. PAN3 encodes a subunit of the Pab1p-dependent poly(A) nuclease in Saccharomyces cerevisiae. Mol. Cell. Biol. (2015). doi:10.1128/mcb.16.10.5744

36. Tharun, S. & Parker, R. Targeting an mRNA for decapping: Displacement of translation factors and association of the Lsm1p-7p complex on deadenylated yeast mRNAs. Mol. Cell (2001). doi:10.1016/S1097-2765(01)00395-1

37. Brouwer, R., Pruijn, G. J. M. & van Venrooij, W. J. The human exosome: An autoantigenic complex of exoribonucleases in myositis and scleroderma. Arthritis Research (2001). doi:10.1186/ar147

38. Andrulis, E. D., Werner, J., Nazarian, A., Erdjument-Bromage, H., et al. The RNA processing exosome is linked to elongating RNA polymerase II in Drosophila. Nature (2002). doi:10.1038/nature01181

39. Allmang, C., Petfalski, E., Podtelejinkov, A., Mann, M., Tollervey, D, Mitchell, P. The yeast exosome and human PM-Scl are related complexes of 3' → 5' exonucleases. Genes Dev. (1999). doi:10.1101/gad.13.16.2148

40. Januszyk, K. & Lima, C. D. The eukaryotic RNA exosome. Current Opinion in Structural Biology (2014). doi: 10.1016/j.sbi.2014.01.011

41. Liu, H., Rodgers, N. D., Jiao, X. & Kiledjian, M. The scavenger mRNA decapping enzyme DcpS is a member of the HIT family of pyrophosphatases. EMBO J. (2002). doi:10.1093/emboj/cdf448

42. Tucker, M. & Parker, R. Mechanisms and Control Of mRNA Decapping in Saccharomyces cerevisiae. Annu. Rev. Biochem. (2002). doi: 10.1146/annurev.biochem.69.1.571

43. Coller, J. & Parker, R. Eukaryotic mRNA Decapping. Annu. Rev. Biochem. (2004). doi: 10.1146/annurev.biochem.73.011303.074032

44. Jinek, M., Coyle, S. M. & Doudna, J. A. Coupled 5' Nucleotide Recognition and Processivity in Xrn1-Mediated mRNA Decay. Mol. Cell (2011). doi: 10.1016/j.molcel.2011.02.004

45. Marchler-Bauer, A., Bo, Y., Han, L., He, Jane., Zheng, C. et al. CDD/SPARCLE: functional classification of proteins via subfamily domain architectures. Nucleic Acids Res. (2016). doi:10.1093/nar/gkw1129

46. Chang, J. H., Xiang, S., Xiang, K., Manley, J. L. & Tong, L. Structural and biochemical studies of the 5'→3' exoribonuclease Xrn1. Nat. Struct. Mol. Biol. (2011). doi:10.1038/nsmb.1984

47. Braun, J. E., Truffault, V., Boland, A., Huntzinger, E., et al. A direct interaction between DCP1 and XRN1 couples mRNA decapping to 5′ exonucleolytic degradation. Nat. Struct. Mol. Biol. (2012). doi:10.1038/nsmb.2413

48. Elbeaino, T., Digiaro, M., Mielke-Ehret, N., Muehlbach, H. P. & Martelli, G. P. ICTV virus taxonomy profile: Fimoviridae. J. Gen. Virol. (2018). doi:10.1099/jgv.0.001143

49. Guo, L., Louis, I. V. S. & Bohjanen, P. R. Viral manipulation of host mRNA decay. Future Virology (2018). doi:10.2217/fvl-2017-0106

50. Chapman, E. G., Moon, S. L., Wilusz, J. & Kieft, J. S. RNA structures that resist degradation by Xrn1 produce a pathogenic dengue virus RNA. Elife (2014). doi:10.7554/eLife.01892

51. Pijlman, G. P., Funk, A., Kondratieva, N., Leung, J., Torres, S., et al. A Highly Structured, Nuclease-Resistant, Noncoding RNA Produced by Flaviviruses Is Required for Pathogenicity. Cell Host Microbe 4, 579–591 (2008). Doi: 10.1016/j.chom.2008.10.007.

52. Funk, A., Truong, K., Nagasaki, T., Torres, S., Floden, N., et al. RNA structures required for production of subgenomic flavivirus RNA. J. Virol. 84, 11407–11417 (2010). Doi: 10.1128/JVI.01159-10

53. Charley, P. A., Wilusz, C. J. & Wilusz, J. Identification of phlebovirus and arenavirus RNA sequences that stall and repress the exoribonuclease XRN1. J. Biol. Chem. (2018). doi:10.1074/jbc.M117.805796

54. Chapman, E. G., Constantino, D., Rabe, J. L., Moon, S. L., Wilusz, J. et al. The structural basis of pathogenic subgenomic flavivirus RNA (sfRNA) production. Science (307-310). (2014). doi:10.1126/science.1250897

55. Moon, S. L., Anderson, J. R., Kumagai, Y., Wilusz, C. J, Akira, S., Khromykh, A. A., Wilusz, J., A noncoding RNA produced by arthropod-borne flaviviruses inhibits the cellular exoribonuclease XRN1 and alters host mRNA stability. RNA 18, 2029–2040 (2012). Doi: 10.1261/rna.034330.112

56. Charley, P. A. & Wilusz, J. Sponging of cellular proteins by viral RNAs. Current Opinion in Virology (2014). doi: 10.1016/j.coviro.2014.09.001

57. Flobinus, A., Chevigny, N., Charley, P. A., Siessler, T., et al. Beet Necrotic Yellow Vein Virus Noncoding RNA Production Depends on a 5'→3' Xrn Exoribonuclease Activity. Viruses 10, 137 (2018). Doi: 10.3390/v10030137

58. Steckelberg, A.-L., Akiyama, B. M., Constantino, D. A., Sit, T. L., Nix, J. C., Kieft, J. S., A folded viral noncoding RNA blocks host cell exoribonucleases through a conformationally dynamic RNA structure. Proc. Natl. Acad. Sci. (2018). doi:10.1073/pnas.1802429115

59. Moon, S. L. Blackington, J. G., Anderson, J. R., Dozier, M. K., Dodd, B. J., et al. XRN1 Stalling in the 5' UTR of Hepatitis C Virus and Bovine Viral Diarrhea Virus Is Associated with Dysregulated Host mRNA Stability. PLoS Pathog. (2015). doi: 10.1371/journal.ppat.1004708

60. Kieft, J. S. Viral IRES RNA structures and ribosome interactions. Trends in Biochemical Sciences (2008). doi: 10.1016/j.tibs.2008.04.007

61. Lukavsky, P. J. Structure and function of HCV IRES domains. Virus Res. (2009). doi: 10.1016/j.virusres.2008.06.004

62. Wilson, J. E., Powell, M. J., Hoover, S. E. & Sarnow, P. Naturally Occurring Dicistronic Cricket Paralysis Virus RNA Is Regulated by Two Internal Ribosome Entry Sites. Mol. Cell. Biol. (2002). doi:10.1128/mcb.20.14.4990-4999.2000

63. Kerr, C. H., Ma, Z. W., Jang, C. J., Thompson, S. R. & Jan, E. Molecular analysis of the factorless internal ribosome entry site in Cricket Paralysis virus infection. Sci. Rep. (2016). doi:10.1038/srep37319

64. Kühn, R., Luz, N., Beck, E., Functional Analysis of the Internal Translation Initiation Site of Foot-and-Mouth Disease Virus. Journal Virol. Vol. 64(10) (4625-4631) (1990).

65. Pelletier, J. & Sonenberg, N. Internal initiation of translation of eukaryotic mRNA directed by a sequence derived from poliovirus RNA. Nature (1988). doi:10.1038/334320a0

66. Kieft, J. S., Zhou, K., Jubin, R. & Doudna, J. A. Mechanism of ribosome recruitment by hepatitis C IRES RNA. RNA (2001). doi:10.1017/S1355838201001790

67. Pestova, T. V., Shatsky, I. N., Fletcher, S. P., Jackson, R. J. & Hellen, C. U. T. A prokaryotic-like mode of cytoplasmic eukaryotic ribosome binding to the initiation codon during internal translation initiation of hepatitis C and classical swine fever virus RNAs. Genes Dev. (1998). doi:10.1101/gad.12.1.67

68. Spahn, C. M. T., Kieft, J. S., Grassucci R. A., Penczek, P. A., Zhou, K., Doudna J. A., Frank, J., Hepatitis C virus IRES RNA-induced changes in the conformation of the 40S ribosomal subunit. Science (1959-1962). (2001). doi:10.1126/science.1058409

69. Fraser, C. S., Doudna, J. A., Leary, J., Yu, Y. & Ji, H. Coordinated assembly of human translation initiation complexes by the hepatitis C virus internal ribosome entry site RNA. Proc. Natl. Acad. Sci. (2004). doi:10.1073/pnas.0407402101

70. Otto, G. A. & Puglisi, J. D. The pathway of HCV IRES-mediated translation initiation. Cell (2004). doi: 10.1016/j.cell.2004.09.038

71. Russo, J. & Wilusz, J. Trick or TREAT: A Scary-Good New Approach for Single-Molecule mRNA Decay Analysis. Molecular Cell (2017). doi: 10.1016/j.molcel.2017.10.027

72. Horvathova, I., Voigt, F., Kotrys, A. V., Zhan, Y., Artus-Revel, C. G., et al. The Dynamics of mRNA Turnover Revealed by Single-Molecule Imaging in Single Cells. Mol. Cell (2017). doi: 10.1016/j.molcel.2017.09.030

73. Boehm, V., Gerbracht, J. V., Marx, M. C. & Gehring, N. H. Interrogating the degradation pathways of unstable mRNAs with XRN1-resistant sequences. Nat. Commun. (2016). doi:10.1038/ncomms13691

74. Barrett, L. W., Fletcher, S. & Wilton, S. D. Regulation of eukaryotic gene expression by the untranslated gene regions and other non-coding elements. Cellular and Molecular Life Sciences (2012). doi:10.1007/s00018-012-0990-9

75. Bidet, K., Dadlani, D. & Garcia-Blanco, M. A. G3BP1, G3BP2 and CAPRIN1 are required for translation of interferon stimulated mRNAs and are targeted by a dengue virus non-coding RNA. PLoS Pathog. 10, e1004242–e1004242 (2014). doi: 10.1371/journal.ppat.1004242

76. Chang, R. Y., Hsu, T. W., Chen, Y. L., Liu, S. F., Tsai Y. J., Lin, Y. T., Chen, Y. S., Fan, Y. H., Japanese encephalitis virus non-coding RNA inhibits activation of interferon by blocking nuclear translocation of interferon regulatory factor 3. Vet. Microbiol. (2013). doi: 10.1016/j.vetmic.2013.04.026

77. Moon, S. L., Dodd, B. J., Brackney, D. E., Wilusz, C. J., Ebel, G. D., Wilusz, J. Flavivirus sfRNA suppresses antiviral RNA interference in cultured cells and mosquitoes and directly interacts with the RNAi machinery. Virology 485, 322–329 (2015). doi: 10.1016/j.virol.2015.08.009

78. Summer, H., Grämer, R. & Dröge, P. Denaturing Urea Polyacrylamide Gel Electrophoresis (Urea PAGE). J. Vis. Exp. (2009). doi:10.3791/1485

79. Petrov, A., Tsa, A. & Puglisi, J. D. Analysis of RNA by analytical polyacrylamide gel electrophoresis. in Methods in Enzymology (2013). doi:10.1016/B978-0-12-420037-1.00016-6

80. Moon, S. L. & Wilusz, J. Cytoplasmic viruses: rage against the (cellular RNA decay) machine. PLoS Pathog. 9, e1003762–e1003762 (2013).

81. Akiyama, B. M., Laurence, H. M., Massey, A. R., Constantino, D. A., Xie, X., Zika virus produces noncoding RNAs using a multi-pseudoknot structure that confounds a cellular exonuclease. Science (1148-1152). (2016). doi:10.1126/science. aah3963

82. Decker, C. J. & Parker, R. A turnover pathway for both stable and unstable mRNAs in yeast: Evidence for a requirement for deadenylation. Genes Dev. 7, 1632–1643 (1993). doi: 10.1101/gad.7.8.1632

83. Couttet, P., Fromont-Racine, M., Steel, D., Pictet, R. & Grange, T. Messenger RNA deadenylation precedes decapping in mammalian cells. Proc. Natl. Acad. Sci. (1997). doi:10.1073/pnas.94.11.5628

84. Chang, R. Y., Hsu, T. W. Chen, Y. L. Liu, S. F., Tsai, Y. J., Lin, Y. T., Chen, Y. S., Fan, Y. H., Japanese encephalitis virus non-coding RNA inhibits activation of interferon by blocking nuclear translocation of interferon regulatory factor 3. Vet. Microbiol. 166, 11–21 (2013). doi: 10.1016/j.vetmic.2013.04.026

85. Wang, C., Le, S. Y., Ali, N. & Siddiqui, A. An RNA pseudoknot is an essential structural element of the internal ribosome entry site located within the hepatitis C virus 5' noncoding region. RNA 1(5) 526-537 (1995).

86. Moes, L. & Wirth, M. The internal initiation of translation in bovine viral diarrhea virus RNA depends on the presence of an RNA pseudoknot upstream of the initiation codon. Virol. J. (2007). doi:10.1186/1743-422X-4-124

87. Hellen, C. U. T. & Sarnow, P. Internal ribosome entry sites in eukaryotic mRNA molecules. Genes and Development (2001). doi:10.1101/gad.891101

88. Jan, E. Divergent IRES elements in invertebrates. Virus Res. (2006). doi: 10.1016/j.virusres.2005.10.011

89. Jan, E. & Sarnow, P. Factorless ribosome assembly on the internal ribosome entry site of cricket paralysis virus. J. Mol. Biol. (2002). doi:10.1016/S0022-2836(02)01099-9

90. Nishiyama, T. et al. Structural elements in the internal ribosome entry site of Plautia stali intestine virus responsible for binding with ribosomes. Nucleic Acids Res. (2003). doi:10.1093/nar/gkg336

91. Pfingsten, J. S., Costantino, D. A. & Kieft, J. S. Structural basic for ribosome recruitment and manipulation by a viral IRES RNA. Science (2006). doi:10.1126/science.1133281

92. Hertz, M. I. & Thompson, S. R. Mechanism of translation initiation by Dicistroviridae IGR IRESs. Virology (2011). doi: 10.1016/j.virol.2011.01.005

93. Kieft, J. S., Zhou, K., Jubin, R., Murray, M, G., Lau, J., Y., Doudna, J., A., The hepatitis C virus internal ribosome entry site adopts an ion-dependent tertiary fold. J. Mol. Biol. (1999). doi:10.1006/jmbi.1999.3095

94. Brown, E. A., Zhang, H., Ping, L. hua & Lemon, S. M. Secondary structure of the 5′ nontranslated regions of hepatitis C virus and pestivirus genomic RNAs. Nucleic Acids Res. (1992). doi:10.1093/nar/20.19.5041

95. Pilipenko, E. V., Gmyl. A., P., Maslova, S., V., Belov, G., A., Sinyakov, A., N., Huang, M., Brown, T., D., Agol V., I., Starting window, a distinct element in the cap-independent internal initiation of translation on picornaviral RNA. J. Mol. Biol. (1994). doi:10.1006/jmbi.1994.1516

96. Jang, S. K. Krausslich, H. G., Nicklin, M, J., Duke, G. M., Palmenberg, A. C., Wimmer, E., A segment of the 5' nontranslated region of encephalomyocarditis virus RNA directs internal entry of ribosomes during in vitro translation. J. Virol. 62(8) 2636-2643 (1988).

97. Borman, A. & Jackson, R. J. Initiation of translation of human rhinovirus RNA: Mapping the internal ribosome entry site. Virology 188, 685–696 (1992). doi:10.1016/0042-6822(92)90523-R

98. Hatakeyama, Y., Shibuya, N., Nishiyama, T. & Nakashima, N. Structural variant of the intergenic internal ribosome entry site elements in dicistroviruses and computational search for their counterparts. RNA (2004). doi:10.1261/rna.5208104

99. Pisarev, A. V Chard, L. S., Kaku, Y., Johns, H, L., Shatsky, I., N., Belsham, G. J., Functional and Structural Similarities between the Internal Ribosome Entry Sites of Hepatitis C Virus and Porcine Teschovirus, a Picornavirus. J. Virol. (2004). doi:10.1128/JVI.78.9.4487

100. Mari, J., Poulos, B. T., Lightner, D. V. & Bonami, J. R. Shrimp Taura syndrome virus: Genomic characterization and similarity with members of the genus Cricket paralysis-like viruses. J. Gen. Virol. (2002). doi:10.1099/0022-1317-83-4-915

101. Shi, G. & Suzuki, T. Molecular basis of encapsidation of Hepatitis C virus genome. Frontiers in Microbiology (2018). doi:10.3389/fmicb.2018.00396

102. Shi, G., Ando, T., Suzuki, R., Matsuda, M., Nakashima, K., et al. Involvement of the 3' Untranslated Region in Encapsidation of the Hepatitis C Virus. PLoS Pathog. (2016). doi: 10.1371/journal.ppat.1005441

103. Henke, J. I., Goergen, D., Zheng, J., Song, Y., Schuttler, C. G., Fehr, C., Junemann, C., Niepmann, M., microRNA-122 stimulates translation of hepatitis C virus RNA. EMBO J. (2008). doi:10.1038/emboj.2008.244

104. Jopling, C. L. Regulation of hepatitis C virus by microRNA-122. *Biochemical Society Transactions* **36,** 1220–1223 (2008).